Received 19 February 2022; accepted 20 March 2022. Date of publication 24 March 2022; date of current version 1 April 2022.

Digital Object Identifier 10.1109/OJCOMS.2022.3162142

Control of Electromagnetic Radiation on Coexisting Smart Radio Environment

MEHMET MERT ŞAHIN [1] (Graudate Student Member, IEEE), HÜSEYIN ARSLAN [1,2] (Fellow, IEEE), AND KWANG-CHENG CHEN [1] (Fellow, IEEE)

[1]Department of Electrical Engineering, University of South Florida, Tampa, FL 33620, USA

[2]Department of Electrical and Electronics Engineering, Istanbul Medipol University, 34810 Istanbul, Turkey

CORRESPONDING AUTHOR: M. M. ŞAHIN (e-mail: mehmetmert@usf.edu)

The work of Hüseyin Arslan was supported by the U.S. National Science Foundation under Award ECCS-1923857.
The work of Kwang-Cheng Chen was supported by Cyber Florida.

ABSTRACT Efficient spectrum utilization is always the fundamental challenge of mobile communication technology toward 6G. Instead of conventional spectral efficiency in bps/Hz, geographical region shall be brought into consideration in bps/Hz/unit-area, which suggests spatial domain technology as a generalization of conventional MIMO to elevate next generation mobile communication technology. Therefore, this paper introduces the formation of smart radio environment considering efficient utilization of radio spectrum in any given geographical area, which can be also viewed as a generalization of cognitive radio technology. By smart management of reconfigurable intelligent surface (RIS) and ambient backscatter communication (ABC) technologies, smart radio environment can be formed in any given area to achieve spectral-spatial efficiency. In this paper, the control of electromagnetic spatial radiation over a region is explored by utilizing repositionable dynamic RIS and harmony of multiple ABC nodes assisted with machine learning (ML) based control mechanism to form spectrum map. Such smart and reconfigurable radio technology demonstrates the superiority of mutual usage of RIS and ABC in terms of shaping the electromagnetic energy in coexisting radio systems. First, the use of multiple RISs is studied to enhance the capacity of secondary use inside the specific area by shaping the electromagnetic energy in the spatial domain. Secondly, a new degree of freedom with repositionable dynamic RIS is introduced. Controlling the time varied shadowing effects by re-positioning the RIS, it is shown that 15% more capacity can be achieved. Finally, the use of multiple coordinated ABCs to protect the region of primary use against the radiation due the secondary uses is investigated. Having coordinated network with repositionable dynamic RIS and multiple ABCs allow us to shape the electromagnetic wave in spatial domain by creating radiation rejection and coverage extension zones. A centralized or distributed mechanism to construct the spectrum map based on ABC sensor is also introduced to instruct existing repositionable dynamic RISs for better coverage. Merging these promising technologies will pave the way for the smart radio environment creating high spectral efficient wireless systems.

INDEX TERMS Coexistence, cognitive radio, spatial-spectral efficiency, reconfigurable intelligent surface, ambient backscatter communications, interference management, smart radio environment.

I. INTRODUCTION

THE 5G wireless networks is proposed to enable three imperative service applications which are massive machine type communications (mMTC), enhanced-mobile broadband (eMBB), and ultra reliable and low latency communications (uRLLC). With the recent developments on key 5G technologies such as massive MIMO, polar coding, cloud radio access network (C-RAN), and so on, the theoretical gain is achieved to be validated by the field test [1]. However, as intelligence, autonomy and ubiquity of digital

word exponentially grow, 5G wireless networks will not be adequate to meet high demand of future applications that need connection of everything consisting of people, vehicles, UAVs, satellites, sensors, data clouds, computing devices and robotic agents [2].

A. VISION FOR 6G

It is expected that 6G wireless networks will fulfill the fully connected digital world and provide ubiquitous wireless connectivity for all. It will open a new era of Internet of intelligence with connected everything [3]. With the emerge of holographic teleportation, increased industrial automation and connection density, next generation 6G systems are needed to possess Tbps-level data rates, microsecond-level latency, improved energy efficiency [4]. Also, industrial Internet of Things (IIoT) concept requires wireless networks guaranteeing spatial reconfigurability and ultra-reliability [5]. With the diverse requirements of emerging applications and use cases, it is believed that 6G systems is intended to enhance the awareness of the whole communication networks including wireless medium and end-points [6]. Such massively connected network needs to have capabilities of real-time learning and data processing for network edges, air interface and user elements that can be enabled via machine learning (ML) [7].

The increase in the number of wireless devices that is expected to reach 125 billion devices all over the world by 2030 [2] and the aim of 1Gb/s/m^2 area traffic capacity [8] boost the importance of spectrum utilization for the next generation wireless systems in the highly overloaded coexisting scenarios. Also, current wireless communication systems cannot provide services to half of the world's population living in remote areas [9] where next generation systems are planned to guarantee at least 10 Mbps by extending the coverage area. Therefore, the electromagnetic radiation emitting from numerous wireless devices serving various applications needs to be controlled intelligently both in the transceiver ends and along the wireless medium. Therefore ultra-advanced spectrum usage and management schemes in licensed and unlicensed band need to embrace all disruptive and smart technologies such as reconfigurable intelligent surface (RIS), ambient backscatter communication (ABC) and ML.

B. SHIFTING FROM COGNITIVE RADIO TO SMART RADIO ENVIRONMENT

Since the birth of cognitive radio by Mitola and Maguire [10] and the extreme success of co-existing wireless systems (e.g., WiFi, Bluetooth, and other devices), wireless technology could dynamically utilize the spectrum and high-spectral waveforms by mitigating interference to primary passive/active uses [11]. Cognitive radio networking (CRN) emerges as an effective way to design the coexisting wireless communication systems offering potential for enhanced spectrum efficiency, interference mitigation and interoperability [12]. (CRN) only controls the parameters of end-to-end radios by sensing the environment and smartly adjusting relevant transmission and reception parameters [13]. Beside cognitive capabilities on the transmitter and receiver end, effective co-existing wireless communication systems demand a disruptive system design and radio frequency (RF) implementation to maximize the spectrum utilization by keeping extremely high radio rejection to avoid interference [14]. For example, in the light of many potential co-existing frequency bands such as those for commercial radio communication reception whose signal strength may be around -70 dBm to -120 dBm and advanced interference mitigation techniques over the whole area are needed to capture the signal safely. Such a technology challenge, which leads to controlling radio radiation on a geographical area, has not been well addressed in literature or engineering patents beyond personal area. Also, how to maximally utilize the spatial spectrum and radiation control according to traffic dynamics in time and spatial domains remains the key challenge for future application scenarios that require high capacity (e.g., holography, virtual reality, non-terrestrial communication), high density (e.g., IoT environment in smart factories and smart offices) and high precision (e.g., robotic assembly and warehouse stocktaking).

Shaping the radiation energy and nulls over the region, together with time, frequency, code domains presents a holistic approach toward smart and reconfigurable radio environments, for more effective spatial spectrum utilization of co-existing wireless systems and networks. A fundamental question arises on how to evolve into coexisting wireless system from spectrum efficiency perspective by taking network infrastructure design into consideration [11]. To answer that, the paradigm of smart radio environment is firstly introduced in [15] and detailed in [16] which is empowered by the RIS. It is motivated that future wireless networks necessitate a smart radio environment with RIS which are capable of sensing the environment and of applying customized transformations to the electromagnetic radio waves. Also, smart radio environments provides more degrees of freedom by electronically controlling the environment itself rather than transmitter and receiver end points and turns the wireless medium into software-reconfigurable entity [17]. Secure wireless transmission, interference reduction, transmission range extension can be considered as some of smart radio environment applications [18].

In this paper, the smart radio environment concept is enriched with the harmony of multiple repositionable dynamic RISs and coordinated ABCs to extend the geographical coverage (by eliminating spectrum holes) and maximize the sum rate throughput for a given geographical region and a given spectrum, while enhancing geographical isolation and minimizing the interference of underlay coexisting cognitive radio networks. In addition to providing controllable reflection properties with RISs [19], [20] and ABC nodes [21], the mobility of these devices in the environment is proposed to further enhance the system performance. The proposed coexisting smart radio environment strategy illustrated by

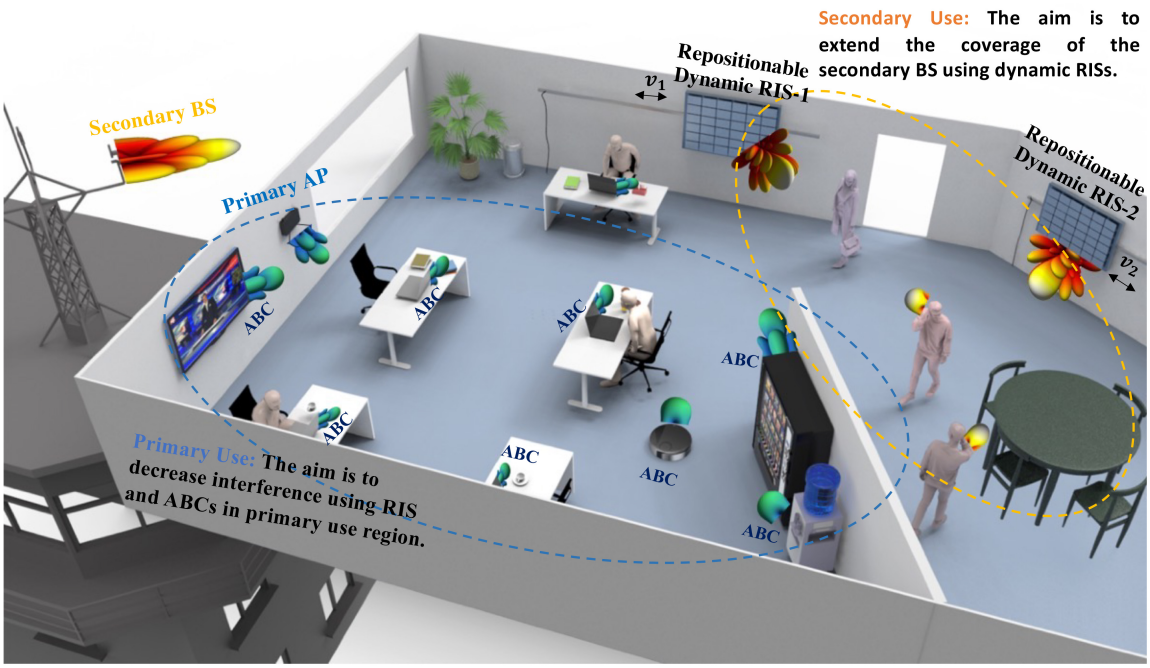

FIGURE 1. Shaping the electromagnetic energy using repositionable dynamic RISs and ABC nodes. ABC nodes are designed to be application specific devices. RISs may operate across in a wide frequency band regime for coarse tuning the radiation of secondary systems.

Fig. 1 will achieve multiple goals including interference management, coverage improvement, enhanced radio environment awareness (REA), effective spectrum mapping and intentional geographical radio isolation that could potentially revolutionize the spatial spectrum efficiency of systems migrating from 5G's C-RAN and massive MIMO to 6G.

C. CONTRIBUTION AND ORGANIZATION OF THE ARTICLE

This research aims to enable smart radio environment by merging two appealing technologies repositionable dynamic RIS and ABC, that helps to maximize the spatial spectrum utilization for cognitive radio systems where two different wireless system applications called primary and secondary uses are present as shown in Fig. 1. The main contributions of the study can be summarized as follows.

- The smart radio environment system is proposed utilizing repositionable dynamic RIS and multiple coordinated ABC to control spatial electromagnetic radiation by creating radiation rejection and coverage extension zones.
- To the best of our knowledge, it is novelly introduced that the repositionable dynamic RISs are utilized to extend the coverage of co-existing secondary systems and coarse radiation rejection for primary systems by having much more control on the exploitation of channel clusters as well as shadowing effects that may causes high power fluctuations in a short time frame.
- It is also first time that a group of coordinated ABC nodes are proposed to create man-made deep fades which greatly reduce the interference from secondary use into the radiation rejection zone hosting primary passive and active uses.
- Construction of spectrum map by cross-layer RF design and support vector machine (SVM) based on 1-bit spectrum sensor data is introduced by novel reusing of ABC to transmit the data to distributed fusion center (DFC).
- The coexistence of all proposed concepts is studied with joint optimization of coverage extension area and radiation rejection zone using both repositionable dynamic RIS and multiple ABCs. Alternation optimization technique is utilized by subgrouping the general problem into smaller ones. The convergence of the proposed technique is evaluated with numerical study as well.

The unique rationale of this study is therefore to create extended, controlled radiation of the secondary systems in the 2D/3D geographical area as shown in the Fig. 1, while creating the radiation-rejection zone to ensure the successful operation of the primary systems. The system architecture of the proposed coexisting wireless communications can be visualized in Fig. 2. As extremely large antenna arrays approaching the limit of massive MIMO, the aim is to steer electromagnetic radiation while creating man-made radio rejection to protect primary passive or active uses. Such a system architecture has a large-scale antenna-array for an access point (AP) or base station (BS), while smaller-scale antenna arrays tagged to each user equipment or smart machine (e.g., robot or autonomous vehicle) which function as backscatterer to create a radiation rejection zone. Moreover, multiple repositionable dynamic RISs advanced by RF/antenna techniques to extend and tailor the geographical coverage (in reliability and outage), such that the

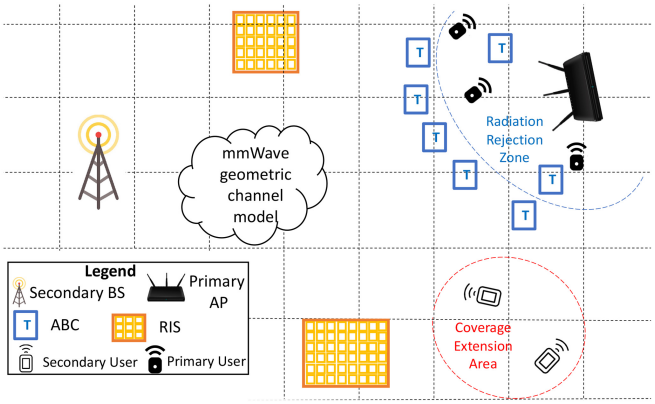

FIGURE 2. System structure including multiple RISs for coverage extension, multiple coordinated ABCs for radiation rejection.

interference to/from the underlay coexisting radio systems can be minimized. Multiple coordinated ABC nodes for fine-tuning of radio coverage by forming radiation rejection to avoid interference to sensitive primary passive/active uses, which is named as virtual region and circled with red curve in Figure 2. The mmWave geometric channel model is utilized to demonstrate the feasibility of the system architecture, where signal-to-noise ratio (SNR) and capacity performance on the measurement points (MPs), which are distributed in the whole geometry, are numerically calculated. In the presented numerical studies, it is shown that these mechanisms allow to create regional shapes where radiated power is distributed as desired. In Section II, it is demonstrated that at least 5 dB increase can be obtained in the power of secondary system along the specific region by introducing multiple static coordinated RIS. Moreover, Section III represents the superiority of repositionable dynamic RIS with the increment of nearly 15% in the capacity of the secondary system. Additionally, simulation results in Section IV demonstrates that the use of coordinated multiple ABC nodes provides nearly 10 dB interference rejection in the vicinity of primary user. Section V merges the proposed architectures into one system and optimizes the parameters to enable smart radio environment having radiation rejection and coverage extension zones at the same time. The use of SVM to spatially identify the secondary communication area by 1-bit data transmitted from ABC sensor is illustrated in Section VI. Finally, future research direction and challenges are presented in Section VII.

II. MULTIPLE RIS TO EXTEND THE COVERAGE OF SECONDARY SYSTEMS

A. STATE OF THE ART

The millimeter wave (mmWave) band usage is significantly investigated regarding next-generation wireless communications [22], which allows very small form-factor antenna arrays for both BS and the user equipments (UEs) [23] and provides highly efficient directional transmissions to meet the high capacity demand of future wireless technologies [24]. However, energy losses in mmWave band channel are more susceptible to the propagation distance compared to the classical sub-3 GHz band [25]. The prominent technology, RIS, is proposed as a channel control mechanism which converts the channel from a problem into a design elements [26]. It can achieve a controlled and narrower beams at larger sizes relative to the wavelength [27] in order to overcome the energy loss problem in mmWave channels. Unlike relays, RIS consumes no energy resulting in less noise effect. However, as shown in a comparison of RIS to decode and forward relaying in [28], RIS is required to have many elements to outperform relaying since it has no power source. In both the RIS and multiple-antenna systems, one major challenge is the channel estimation and synchronization due to the large number of passive elements in a RIS. However, the sparseness of mmWave channels allows feasible and efficient synchronization and channel estimation algorithms. Using few active elements along the RIS for channel estimation is proposed in [29], and after estimating the channel, these active elements turn back to the reflecting mode again. For instance, a two stages algorithm is proposed in [30] for multi-user communication, where all elements are turned off firstly, and the channel between BS and users is estimated. Secondly, the RIS elements are turned on one by one and the channel of all users is estimated for that element. The full reflection of the RIS is considered at all time, i.e., all of its elements are switched ON with maximum reflection amplitude during both the channel estimation and data transmission phases [31]. It is inevitable fact that as the channel estimation and optimization schemes of the RIS develop, the usage of the RIS in modern wireless systems will expand.

B. SYSTEM MODEL

The RIS smartly controls the radio environment by scattering the signals to mitigate pathloss, fading, blockage, and multipath effects. It is typically configured to direct the primary system signal towards the destination by adapting its antenna elements to the propagation environment, while being regarded as nearly passive elements without any need for amplifiers or analog-to-digital/digital-to-analog converters (ADCs and DACs). This research disruptively utilizes the RIS to extend the coverage area of secondary systems and to decrease the interference in the vicinity of primary systems as the goal of Fig. 1. To extend the coverage of secondary active uses, two RISs are illustrated to create the smart radio environment in Fig. 2. To protect the zone which can be passive or active primary use, multiple ABCs are placed around the primary use area.

Omnidirectional pathloss at the distance d is estimated using the d_0 reference distance for the antenna far-field as follows [32]:

$$\mathrm{PL}(d)[\mathrm{dB}] = \mathrm{PL}(d_0) + 10\bar{n}\log_{10}\left(\frac{d}{d_0}\right) + \mathrm{SF}, \quad (1a)$$

$$\mathrm{PL}(d_0)[\mathrm{dB}] = 20\log_{10}\left(\frac{4\pi d_0 f_c}{c}\right), \quad (1b)$$

where c is the speed of light, 3×10^8 m/s, f_c in Hz is the carrier frequency, $\bar{n}$ is the path loss exponent, and SF is the shadow factor in dB. The far-field path-loss equation in (1a) is compatible with the pathloss expression given in [33]. Also, outdoor-to-indoor penetration loss is considered assuming the environment has low loss buildings. Therefore, the following parabolic model [34] is used for building penetration loss (BPL):

$$\mathrm{BPL[dB]} = 10\log_{10}\left(5 + 0.03 \cdot f_c^2\right). \tag{2}$$

Throughout the study, the narrow-band mmWave channel model is used. It is assumed that all clusters and multi-path components arrive simultaneously and all their frequency components over the channel bandwidth B are received with the same level of attenuation. The corresponding channel matrix $\mathbf{H} \in \mathbb{C}^{N_r \times N_t}$ at the time instant t is written as follows [25]:

$$\mathbf{H} = \sum_{n_{cl}=1}^{N_{cl}} \sum_{p=1}^{N_p(n_{cl})} \alpha_{n_{cl},p} \cdot \Omega_{n_{cl},p}^{R_x}\left(\psi_{n_{cl},p}^{R_x}, \theta_{n_{cl},p}^{R_x}\right) \cdot \Omega_{n_{cl},p}^{T_x}\left(\psi_{n_{cl},p}^{T_x}, \theta_{n_{cl},p}^{T_x}\right)^H, \tag{3a}$$

$$\left|\alpha_{n_{cl},p}\right|^2 = \epsilon_0 e^{\frac{-T_{n_{\mathrm{cl}}}}{-\Gamma_{n_{\mathrm{cl}}}}} e^{\frac{-\tau_{n_{\mathrm{cl}},p}}{-\Gamma_p}} 10^{-0.1(\mathrm{PL[dB]+BPL[dB]+}Z_{\mathrm{cl}}+U_p)}, \tag{3b}$$

where N_{cl} and $N_p(n_{cl})$ denote the number of clusters and rays per each cluster, respectively. $Z_{\mathrm{cl}} \sim N[0, \sigma_{\mathrm{cl}}]$ and $U_p \sim N[0, \sigma_p]$ denote per-cluster and per-subpath shadowing in dB, respectively. $T_{n_{\mathrm{cl}}}$, $\tau_{n_{\mathrm{cl}},p}$, $\Gamma_{n_{\mathrm{cl}}}$, and Γ_p correspond to cluster arrival time, subpath arrival time, cluster decay constant, and subpath decay constant, respectively. The parameters $\psi_{n_{cl},p}$ and $\theta_{n_{cl},p}$ are pth multi-path component of the n_{cl}th cluster's azimuth and elevation angles, respectively, and they characterize the angle-of-departure (AoD) and angle-of-arrival (AoA) at the transmitter and receiver. Moreover, $\Omega_{n_{cl},p}^{\mathrm{Tx}}$ represents the $N_t \times 1$ array factor (AF) of the transmitter antenna array and $\Omega_{n_{cl},p}^{\mathrm{Tx}}$ represents the $N_r \times 1$ AF of the receiver antenna array. The notation $(\cdot)^H$ refers to the Hermitian transpose. The notations for the RIS presented here are also used to clarify the subsequent sections, as well. Define a diagonal matrix $\mathbf{\Theta}_{\mathrm{RIS}_k} = \mathrm{diag}(\beta_1 e^{j\theta_1}, \ldots, \beta_{n_{\mathrm{RIS}_k}} e^{j\theta_{n_{\mathrm{RIS}_k}}}, \ldots, \beta_{N_{\mathrm{RIS}_k}} e^{j\theta_{N_{\mathrm{RIS}_k}}})$ with $k = 1, \ldots, K$, where K is total number of the RIS deployed in the environment. The notation N_{RIS_k} denotes for the total reflecting elements in the kth RIS, $\beta_{n_{\mathrm{RIS}}}$ is the amplitude reflection coefficient of the n_{RIS}th element of kth RIS and j is the imaginary unit. Throughout the study, the reflection coefficient is assumed to be unit value ($\beta_{n_{\mathrm{RIS}_k}} = 1$), same as in [35]. The b_{RIS}-bit discrete phase shift of RIS antennas can be chosen from the set $\mathcal{F}_{\mathrm{RIS}}$ which is defined as follows [36]:

$$\mathcal{F}_{\mathrm{RIS}} = \left\{\theta_{n_{\mathrm{RIS}_k}} = \frac{\varsigma_{n_{\mathrm{RIS}}}\pi}{2^{b_{\mathrm{RIS}}} - 1} \,\middle|\, \varsigma_{n_{\mathrm{RIS}}} \in \boldsymbol{\varsigma}_{\mathrm{RIS}} = \left\{0, 1, \ldots, 2^{b_{\mathrm{RIS}}} - 1\right\}\right\}. \tag{4}$$

Uniform planar array (UPA) is utilized to represent RISs. Denote I_r and I_c the number of elements along with the row and column of the plane array, then the array response vector becomes [37]

$$\Omega_{UPA}(\psi, \theta) = \left[1, \ldots, e^{jx(i_r \cos(\psi)\cos(\theta) + i_c \sin(\theta))2\pi/\lambda}, \ldots\right], \tag{5}$$

where x is the inter-element spacing. $0 \leq i_r < I_r$ and $0 \leq i_c < I_c$ are the row and column indices of an antenna element, respectively. Analog beamforming is considered at the transmitter antenna array, where N_{BS} is the total number of antennas. Transmitter antenna array is considered as more complex compared to RIS elements, therefore, its phase shifter can generate more options with the control of b_{BS} bits. Then, the phase shift for the n_{BS}th transmit antenna can be chosen from the set $\mathcal{F}_{\mathrm{BS}}$ where

$$\mathcal{F}_{\mathrm{BS}} = \left\{\theta_{n_{\mathrm{BS}_k}} = \frac{\varsigma_{n_{\mathrm{BS}}}\pi}{2^{b_{\mathrm{BS}}} - 1} \,\middle|\, \varsigma_{n_{\mathrm{BS}}} \in \boldsymbol{\varsigma}_{\mathrm{BS}} = \left\{0, 1, \ldots, 2^{b_{\mathrm{BS}}} - 1\right\}\right\}. \tag{6}$$

After the selection of n_{BS}th antenna phase shift the beamforming matrix $\boldsymbol{W}$ is formed with power constraint P. In the smart radio environment, spatial consistency is considered [38] which means that the large fading effects and scattering environment are correlated when multiple MPs are closely located in a local area (e.g., 10-15 m). Section III includes detailed explanation regarding how to integrate spatial consistency into the channel model. It should also be mentioned that perfect channel state information (CSI) is assumed throughout out the study for both RIS and ABC phase shift optimization, which is similar to [39], [40].

C. PROBLEM FORMULATION FOR COVERAGE EXTENSION

In this subsection, the problem formulation to extend the coverage of secondary system via multiple static RISs is derived. In order to perform spatial-domain based simulations, multiple MPs are selected randomly which can be considered as many single antenna receivers. Since the coverage inside the specific area is desired to be increased, these measurement points are selected inside that area. The 2D demonstration of the simulation can be seen in Fig. 3, where the area, whose capacity for the secondary is intended to increase is shown by red circle.

The overall RIS-assisted MIMO system have three main propagation ways which are between Tx and the RIS, the RIS and Rx and direct way, which is assumed as non-line-of-sight (NLOS) channel. Regarding the channel matrices, $\mathbf{H}_{\text{BS-MP}_m}$, $\mathbf{H}_{\text{BS-RIS}_k}$, and $\mathbf{H}_{\text{RIS}_k\text{-MP}_m}$ correspond to the channels between BS and mth MP, BS and kth RIS, kth RIS and mth MP, respectively. Analog beamformer matrix $\mathbf{W} \in \mathbb{C}^{N_{\mathrm{BS}} \times 1}$ is applied at the transmitter antenna array having N_{BS} antennas with total power P. As an example with two RIS, the channel matrices for the mth MP are $\mathbf{H}_{\text{BS-MP}_m} \in \mathbb{C}^{1 \times N_{\mathrm{BS}}}$,

Algorithm 1 Alternating Optimization for (P1)

1: Initialize the all elements of $\mathbf{W}$, and $\theta_{n_{\text{RIS}_k}}$, $1 \leq n_{\text{RIS}_k} \leq N_{\text{RIS}_k}, \forall k = 1, \ldots, K$ with one.
2: **repeat**
3: **for** n $\leq N_{\text{BS}} + \sum_{k=1}^{K} N_{\text{RIS}_k}$ **do**
4: Find the indices $\varsigma_{\text{BS}} \in \boldsymbol{\varsigma}_{\text{BS}}$ and $\varsigma_{\text{RIS}_k} \in \boldsymbol{\varsigma}_{\text{RIS}}$ that maximize the average capacity of total M MPs, which defined as $\mathbb{E}\{\mathbf{R}\}$
5: Assign the corresponding phase shift values depending on the index ς_{BS} or ς_{RIS_k} to the corresponding antenna phase shifter n
6: **end for**
7: **until** Convergence is reached

$\mathbf{H}_{\text{BS-RIS}_1} \in \mathbb{C}^{N_{\text{RIS}_1} \times N_{\text{BS}}}$, $\mathbf{H}_{\text{RIS}_1\text{-MP}_m} \in \mathbb{C}^{1 \times N_{\text{RIS}_1}}$, $\mathbf{H}_{\text{BS-RIS}_2} \in \mathbb{C}^{N_{\text{RIS}_2} \times N_{\text{BS}}}$, and $\mathbf{H}_{\text{RIS}_2\text{-MP}_m} \in \mathbb{C}^{1 \times N_{\text{RIS}_2}}$ where N_{RIS_1} and N_{RIS_2} denote the numbers of elements for the first and second RISs. Moreover, phase matrices are $\boldsymbol{\Theta}_{\text{RIS}_1} \in \mathbb{C}^{N_{\text{RIS}_1} \times N_{\text{RIS}_1}}$, and $\boldsymbol{\Theta}_{\text{RIS}_2} \in \mathbb{C}^{N_{\text{RIS}_2} \times N_{\text{RIS}_2}}$ for the first and second RISs, respectively. The channel gain, G_m, for the mth MP with the presence of total K RISs can be represented as follows [26]:

$$G_m = \left| \mathbf{H}_{\text{BS-MP}_m} \mathbf{W} + \sum_{k=1}^{K} \mathbf{H}_{\text{RIS}_k\text{-MP}_m} \boldsymbol{\Theta}_{\text{RIS}_k} \mathbf{H}_{\text{BS-RIS}_k} \mathbf{W} \right|^2. \quad (7)$$

Assuming transmit power equals to 0dBm, capacity of the mth MP is evaluated by Shannon capacity formula:

$$R_m = B \log_2 \left(1 + \frac{G_m}{\sigma^2} \right), \quad (8)$$

where B is the bandwidth and σ^2 is the variance of independent and identically distributed (i.i.d) circularly symmetric complex Gaussian noise with zero mean. Let $\mathbf{R} = [R_1, R_2, \ldots, R_M]$ and $\boldsymbol{\Theta}_{\text{RIS}} = [\boldsymbol{\Theta}_{\text{RIS}_1}, \ldots, \boldsymbol{\Theta}_{\text{RIS}_K}]$, the optimization problem can be formulated as follows [41]:

$$\begin{aligned} (P1) \quad & \max_{\boldsymbol{\Theta}_{\text{RIS}}, \boldsymbol{W}} \quad \mathbb{E}\{\mathbf{R}\} \\ & \text{s.t.} \quad \|\mathbf{W}\|^2 <= P \\ & \theta_{n_{\text{BS}_k}} \in \mathcal{F}_{\text{BS}}, \quad 1 \leq n_{\text{BS}_k} \leq N_{\text{BS}_k} \\ & \theta_{n_{\text{RIS}_k}} \in \mathcal{F}_{\text{RIS}}, \quad 1 \leq n_{\text{RIS}_k} \leq N_{\text{RIS}_k}, \end{aligned} \quad (9)$$

where $\mathbb{E}$ is the expectation operator over M total MP. As it is studied in [42], the optimization problem (P1) is non-convex. Alternating optimization technique, as it is proposed in [43], is utilized to arrange the phase shifts of the BS and RISs at MPs as a solution to (P1). The procedure of this iterative technique is explained in Algorithm **1**.

D. NUMERICAL RESULTS

The numerical results demonstrates the advantage of deploying multiple static RISs to expand the coverage of the secondary active uses. The 2D topological color map in Fig. 3 shows the performance of RISs compared to BS beamforming in order to maximize the signal power in the red encircled area of 15 MPs in terms of dB. The secondary user (SU) is located at (0, 0) and denoted as black star, whereas the primary user (PU), which is white star, is located at (0, 120). Information about other simulation parameters can be found in Table 1. In Fig. 3a, only BS beamforming is utilized to extend the coverage on the area encircled with red color. Enlarged picture of the encircled region is shown as well. In Fig. 3b, two RISs are denoted as magenta circles which are distributed in the map. MPs use the single-element antenna where phase shifts of RISs are arranged to maximize the average capacity of all MPs as formulated in (P1).

Throughout the mathematical simulations of the study, it is assumed that RISs has two different phase options controlled by one-bit, whereas the phase options for BS antennas are chosen from the six-bit discrete phase-shifter. They all are optimized in an iterative manner until convergence is achieved by Algorithm 1. In this urban-microcell simulation, the BS antenna number is taken as $N = 16$ and the numbers of elements for first RIS and second RIS are 128 and 256, respectively. The signal power in the encircled area by BS beamforming can be seen in Fig. 3a, whereas the effect of RISs can be seen in Fig. 3b. As shown in the enlarged plots, simple usage of two RISs already achieves approximately 6 dB gain regarding the signal power of secondary

TABLE 1. Simulation parameters.

Parameter	Value
Carrier Frequency	28 GHz
Antenna gain of BS	30 dB
Transmitter gain of BS	10 dB
Antenna gain of ABC	15 dB
Operating Scenario	Urban Microcell
BS Antenna Number	16
RISs Element Numbers	128, 256
ABCs Antenna Number	4x4 (both Rx, Tx)
Number of total ABCs	16

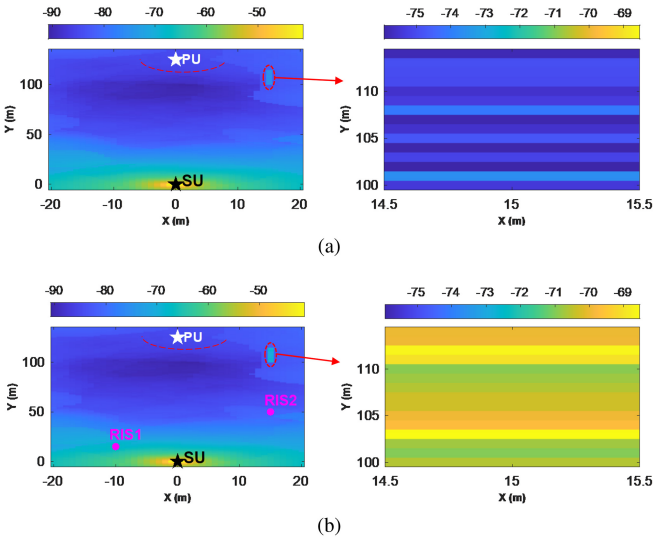

FIGURE 3. Demonstration of coverage extension with two RISs compared with only BS beamforming, (a) only BS to extend coverage, (b) with two RISs to extend coverage where the color map is scaled in dB.

user even if there is 1 bit control on RIS. It is well known that the number of bits in the RIS design, and the location of RIS remarkably affect the performance in the coverage area. These effects are studied in the following section.

III. REPOSITIONABLE DYNAMIC RIS DEPLOYMENT

A. STATE OF THE ART

It is studied that the location, beam alignment, and phase of the RIS can be optimized to enhance the system performance [44], [45]. Although the current RIS technology primarily deploys fixed elements built in the terrestrial scenarios, the integration of RIS into mobile systems gets a lot of interest from the academia. For example, reference [46] studies aerial platforms with RIS and propose a control mechanism for communication, mobility, and sensing. Additionally, joint optimization of active beamforming at the UAV, passive beamforming at the RISs, and UAVs trajectory over a given flying time is studied in [47]. However, locations of the RISs are assumed as fixed and only the movement of UAV is considered. Therefore, the control over the channel clusters is limited.

It is known that glitches occur in the power of "pencil-beam" signal whenever even humans walk across it resulting in a huge SNR drop of 20dB [48]. This scenario can be encountered in shopping malls, office environments and especially IoT factories where tactile Internet plays a very important role. To the best of authors knowledge, a wireless channel control concept based on position adaptive antenna array is firstly introduced by the USF-WAMI team [49], [50] in order to impede detrimental random effects in the wireless channel. In these studies, the concept is implemented via the microfluidically reconfigurable RF devices. Moreover, it is also known that positioning of RIS plays an important role to improve the system performance [51]. However, dynamic positioning of RIS regarding the mobility in the indoor environment hasn't studied yet. Arranging the RIS position dynamically, we will have much more control on exploitation of channel clusters as well as shadowing effects that may causes high power fluctuations in a short time frame. It is believed that the repositionable dynamic RIS will shed a light on how to solve these problems and introduce additional degree of freedom.

Applying repositionable dynamic RIS, the channel control could be more efficient by placing the RIS elements at the optimal location. In addition to the phases of the RIS elements, the location of the surface needs to be optimized. For mobile and nomadic users, the optimal location changes over time, requiring repositionable dynamic RIS deployment. As the scenario in Fig. 1 depicts, more than one repositionable dynamic RISs with a simple rail-based moving system will be implemented to examine the superiority of repositionable dynamic RISs, in terms of spectrum utilization and interference management.

The position of RIS may be initially changed along the linear line in the range of approximately five meters with a slow speed (in the scale of seconds). Since its position will change along the one dimension and the geometry of RIS elements will be fixed, tracking and channel estimation process (or equivalent synchronization) will be practical to implement and deployment compared to 3D movement in spatially adaptive antenna arrays.

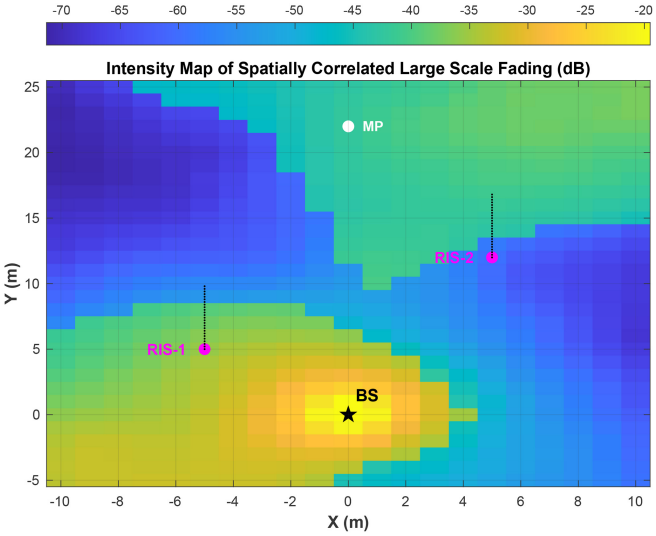

FIGURE 4. Demonstration for the power distribution regarding shadowing and path-loss effects. Initial RISs locations and their trajectories are shown as magenta circle, and black dashed line, respectively.

B. METHODOLOGY

To realize the spatial consistency while re-positioning the RIS, spatially correlated large-scale parameters such as SF (shadow fading), line-of-sight (LOS)/non-LOS (NLOS) condition are generated [38]. The correlation distance in indoor simulation is determined as 5 meter [52]. In addition to point-to-point channel $\mathbf{H}$ generated in (3a) and (3b), a 2D exponential filter is applied to the simulated area as follows:

$$f(p,q) = \exp\left(-\frac{\sqrt{p^2+q^2}}{d_{\text{co}}}\right), \tag{10}$$

where p and q are filter coordinates with respect to the center of the filter, d_{co} is the correlation distance of shadowing. Applying the filter to the channel $\mathbf{H}$, the correlated values in the map is calculated as follows:

$$\mathbf{H_c}(i,j) = \sum_p \sum_q f(p,q)\mathbf{H}(i-p+1, j-q+1), \tag{11}$$

where $\mathbf{H}_c(i,j)$ is the correlated channel, i and j are the coordinates of grid points in the map M with $(i,j)_k \in \mathbb{R}^2$ for kth RIS. Throughout the study, the movement of the RIS is constrained in only y axis with at most 5 m distance change as it is shown in Fig. 4.

C. PROBLEM FORMULATION TO CONTROL CHANNEL CLUSTERS

The aim to deploy repositionable dynamic RIS on the environment is to have a more control on the channel power

variations in a short time frame. It introduces a new degree of freedom, where the speed and location of the RIS can be controlled. Similar to Section II-C, the problem is how to extend the coverage of secondary use in the dedicated area with the help of novel technique, repositionable dynamic RIS.

With the concept of repositionable dynamic RIS, the channel gain evaluated in (7) depends on the position of kth RIS. The location kth RIS of RISs is expressed as 2D pairs, $(i,j)_k, \forall k = 1,\ldots,K$. The channel matrix $\mathbf{H}(i,j)$ at that position is obtained via (11). Then, the channel gain G'_m for the mth MP can be written as follows:

$$G'_m = \Big|\mathbf{H}_{\text{BS-MP}_m}\mathbf{W} + \sum_{k=1}^{K}\mathbf{H}(i,j)_{\text{RIS}_k\text{-MP}_m}\mathbf{\Theta}_{\text{RIS}_k}\mathbf{H}(i,j)_{\text{BS-RIS}_k}\mathbf{W}\Big|^2. \quad (12)$$

One realization of spatially correlated map with two RISs placed in the environment can be seen in Fig. 4. Similar to (8), the capacity of the mth MP with different RISs locations is evaluated as follows:

$$R'_m = B\log_2\left(1+\frac{G'_m}{\sigma^2}\right). \quad (13)$$

The position $(i,j)_k$ of the kth RIS is needed to be considered in the optimization problem (P1), when the repositionable dynamic RIS is studied. By defining the position matrix with $\mathbf{Z} = [(i,j)_1^T,\ldots,(i,j)_K^T]$, and $\mathbf{R}' = [R'_1, R'_2, \ldots, R'_M]$ the problem formulation (P1) can be modified as follows:

$$\begin{aligned}(P2)\quad \max_{\mathbf{\Theta}_{\text{RIS}},\mathbf{W},\mathbf{Z}}\ & \mathbb{E}\{\mathbf{R}'\}\\ \text{s.t.}\ & \|\mathbf{W}\|^2 <= P\\ & \theta_{n_{\text{BS}_k}} \in \mathcal{F}_{\text{BS}},\quad 1 \le n_{\text{BS}_k} \le N_{\text{BS}_k}\\ & \theta_{n_{\text{RIS}_k}} \in \mathcal{F}_{\text{RIS}}, 1 \le n_{\text{RIS}_k} \le N_{\text{RIS}_k}\\ & (i,j)_k \in \mathsf{M}. \end{aligned} \quad (14)$$

Similar to Algorithm **1**, exhaustive searching of both the position of RISs and their phase of elements is considered to solve non-convex optimization problem (P2). Detailed algorithm scheme is presented Algorithm **2**.

D. NUMERICAL RESULTS

The advantage of repositionable RIS in terms of capacity can be seen in Fig. 5, considering both 1-bit and 4-bits RIS.

It is observed that approximately 15% improvement in the capacity of secondary system is achieved with the use of repositionable dynamic RIS. Also, the increase in the phase shifter capability helps to enhance the system performance, as well. Throughout the study, it is assumed that the speed of RISs is low enough to neglect the Doppler shifts. However, the time domain representation including time-frequency Doppler shift profile of the received signal and its effect on performance should be studied and more general mobility patterns, including ways of linear and nonlinear motion, should be explored in the future researches.

Algorithm 2 Alternating Optimization for (P2)

1: Initialize the all elements of $\mathbf{W}$, and $\theta_{n_{\text{RIS}_k}}, 1 \le n_{\text{RIS}_k} \le N_{\text{RIS}_k}, \forall k = 1,\ldots,K$ with one. Also, choose arbitrary RISs locations to determine $(i,j)_{\text{RIS}_k}$.
2: **repeat**
3: **for** all grid points $(i,j)_{\text{RIS}_k} \in \mathsf{M}, \forall k = 1,\ldots,K$ **do**
4: **for** n $\le N_{\text{BS}} + N_{\text{RIS}_1} + N_{\text{RIS}_2}$ **do**
5: Find the indices $\varsigma_{\text{BS}} \in \mathbf{\varsigma}_{\text{BS}}$, $\varsigma_{\text{RIS}_k} \in \mathbf{\varsigma}_{\text{RIS}}$, and $(i',j')_{\text{RIS}_k} \in \mathsf{M}$ that maximize the average capacity of total M MPs, which defined as $\mathbb{E}\{\mathbf{R}'\}$
6: Assign the corresponding phase shift values depending on the index ς_{BS} or ς_{RIS_k} to the corresponding antenna phase shifter n
7: **end for**
8: Fix the position of kth repositionable dynamic RIS to the point of $(i',j')_{\text{RIS}_k}$
9: **end for**
10: **until** Convergence is reached

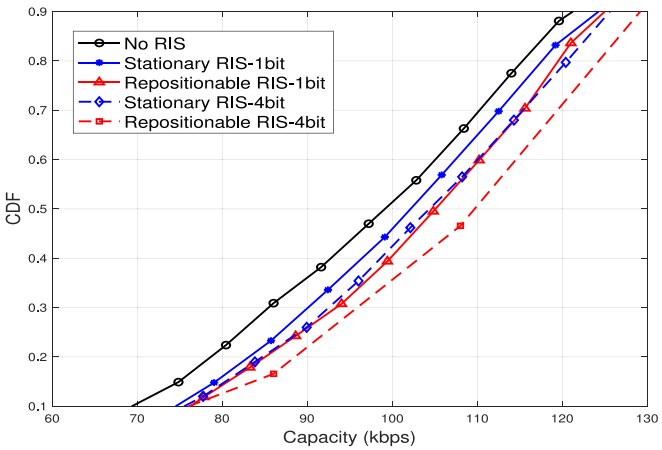

FIGURE 5. Numerical evaluation of capacity of the proposed system showing the advantage of repositionable dynamic RIS.

IV. CREATION OF RADIATION-REJECTION ZONE VIA ABCS

A. STATE OF THE ART

Although the dynamic deployment of RISs can extend the radio coverage of the co-existing system(s), to avoid the interference to the primary system (particularly the receivers of primary system having high radio sensitivity or operating in low signal strength), there are needs for further improved technology beyond effective guided radio coverage by RISs. A disruptive thinking to this technology challenge is to create the *radiation rejection zone* as shown in Fig. 2 against signal transmission from the secondary system. Such radiation rejection zone shall meet the following conditions: (i) further degrading the signal strength from the secondary system into the zone; (ii) minimum interference to the reception of primary system; (iii) the radiation rejection being formed by devices of low energy consumption or battery-less.

To facilitate the disruptive technology forming the radiation rejection zone, considering coherent modulations in state-of-the-art systems, it may disruptively backscatter the signals from secondary system and deploy these nodes just outside the area of desirable radiation rejection zone. The rationale behind is to use each backscatter node to create a new transmission path with appropriate phase change in the nearby area (due to low power), such that creates man-made deep fades of secondary co-existing transmission for nearby receivers of primary use. This disruptive way to apply backscatter technique is simple but surprisingly satisfies desirable conditions.

The ABC is introduced by [53], [54] with little or even no battery power. With the advance of wireless power charging technology, ABCs has received great attention [21] in IoT and sensor networks. Its reservation-based multi-access is studied in [55]. Further explorations based on cooperative communications [56] and cognitive communications [57] suggest wide range of application scenarios. For low-complexity, non-coherent backscatter communication is examined in [58]. All rely on successful RF/antenna implementation. Recently, symbiotic radio (SR) system is proposed to utilize cognitive backscattering communication concept to enhance the reliability and inter-connectivity of ABC devices [59].

B. METHODOLOGY

The concept of creating man-made deep fades to reject radiation from secondary co-existing communication, of course, can not be realized simply by 180° phase inversion at each scattering node, which must be organized into a small antenna array to create meaningful man-made fades. A combination of two beamforming integrated circuit (BFIC) can be used for ABC implementation having two antenna arrays for transmit (Tx) and receive (Rx) functionality. The array can includes both variable 5-bit phase shifter and variable amplifier with the range of 31 dB [60]. Two micro-controller units can arrange both the phase, amplitude and functionality of the ABC antenna array. Actually, thanks to similarity in RIS and ABC, these backscatter nodes together can form the mutual symbiotic wireless system, by reusing earlier mathematical principles regarding the mmWave channel and 2D topographic map generation. Instead of using the RIS, multiple ABCs are placed near the protected zone to collectively form the desirable radiation rejection zone around the sensitive primary receiver as Fig. 2. Particularly, the radiation rejection zone shown inside the red line in Fig. 2 may well serve the protection to primary passive and active uses.

Similar to phase shifter matrix of the RIS explained in the Section II-B, the analog beamforming matrix of lth ABC is defined as $\mathbf{\Theta}_{\mathrm{ABC}_l} = \mathrm{diag}(\beta_1 e^{j\theta_1}, \ldots, \beta_{n_{\mathrm{ABC}_l}} e^{j\theta_{n_{\mathrm{ABC}_l}}}, \ldots, \beta_{N_{\mathrm{ABC}_l}} e^{j\theta_{N_{\mathrm{ABC}_l}}})$, where $l = 1, \ldots, L$ and L is the total number of ABCs operating in the system where each ABC has N_{ABC} antennas. To explore the advantage of deploying multiple ABCs to protect the radiation rejection zone from secondary transmissions, ABCs are first assumed to locate beside the protected zone. Addition to the common channel model explained in the Section II-B, for the mth MP, the matrices $\mathbf{H}_{\text{BS-ABC}_l} \in \mathbb{C}^{N_{\mathrm{ABC}_l} \times N_{\mathrm{BS}}}$, and $\mathbf{H}_{\mathrm{ABC}_l\text{-MP}_m} \in \mathbb{C}^{1 \times N_{\mathrm{ABC}_l}}$ are generated where N_{ABC_l} denotes the antenna number of the lth ABC. The phase matrix of lth ABC is $\mathbf{\Theta}_{\mathrm{ABC}_l} \in \mathbb{C}^{N_{\mathrm{ABC}_l} \times N_{\mathrm{ABC}_l}}$. Similar to transmitter antenna array, phase shifter of ABC generates $2^{b_{\mathrm{ABC}}}$ options with the control of b_{ABC} bits. The phase shift selection for the n_{ABC}th transmit antenna can be chosen from the set $\mathcal{F}_{\mathrm{A}}$ where

$$\mathcal{F}_{\mathrm{A}} = \left\{ \theta_{n_{\mathrm{ABC}_k}} = \frac{\varsigma_{n_{\mathrm{ABC}}} \pi}{2^{b_{\mathrm{ABC}}} - 1} \,\middle|\, \varsigma_{n_{\mathrm{ABC}}} \in \boldsymbol{\varsigma}_{\mathrm{ABC}} = \left\{ 0, \ldots, 2^{b_{\mathrm{ABC}}} - 1 \right\} \right\}. \tag{15}$$

The channel gain from the secondary user transmission for the mth MP, G''_m, can be written as follows:

$$G''_m = \left| \mathbf{H}_{\text{BS-MP}_m} \mathbf{W} + \sum_{l=1}^{L} \mathbf{H}_{\mathrm{ABC}_l\text{-MP}_m} \mathbf{\Theta}_{\mathrm{ABC}_l} \mathbf{H}_{\text{BS-ABC}_l} \mathbf{W} \right|^2, \tag{16}$$

where the total L number ABCs located in the vicinity of primary user. The interference power in m the MP around the primary user region due to secondary user transmission is equal to G''_m.

C. PROBLEM FORMULATION FOR NULLING THE ZONES

Here, the aim for using multiple coordinated ABCs is to reject the radiation due to secondary transmission in the vicinity of primary use. The electromagnetic energy is shaped via backscattering phenomena to protect the primary use zone from unwanted and detrimental radiation. It is shown in the numerical results that by coordinating every ABC nodes, the zone which is protected from primary user radiation can be created.

Letting $\mathbf{G}'' = [G''_1, \ldots, G''_M]$ and $\mathbf{\Theta}_{\mathrm{ABC}} = [\mathbf{\Theta}_{\mathrm{ABC}_1}, \ldots, \mathbf{\Theta}_{\mathrm{ABC}_L}]$, the optimization problem aiming to create radiation rejection zone can be formulated as minimization problem [60]:

$$\begin{aligned} (P3) \quad & \min_{\mathbf{\Theta}_{\mathrm{ABC}}, \mathbf{W}} \ \mathbb{E}\{\mathbf{G}''\} \\ & \text{s.t.} \ \ \|\mathbf{W}\|^2 <= P \\ & \theta_{n_{\mathrm{BS}_k}} \in \mathcal{F}_{\mathrm{BS}}, \ 1 \le n_{\mathrm{BS}_k} \le N_{\mathrm{BS}_k} \\ & \left\| \mathbf{\Theta}_{\mathrm{ABC}_l} \right\|^2 <= P_l, \quad 1 \le l \le L, \\ & \theta_{n_{\mathrm{ABC}_k}} \in \mathcal{F}_{\mathrm{A}}, 1 \le n_{\mathrm{ABC}_k} \le N_{\mathrm{ABC}_k} \end{aligned} \tag{17}$$

where P_l is the power constraint of the lth ABC. Similar to Algorithm **1** and Algorithm **2**, alternating optimization technique is again utilized to arrange the phase shifts at the BS, and ABCs of 5-bit discrete phase-shifters. The aim of the optimization algorithm for the problem (P3) is instead to minimize the average interference power in the area of secondary use, $\mathbb{E}\{\mathbf{G}''\}$.

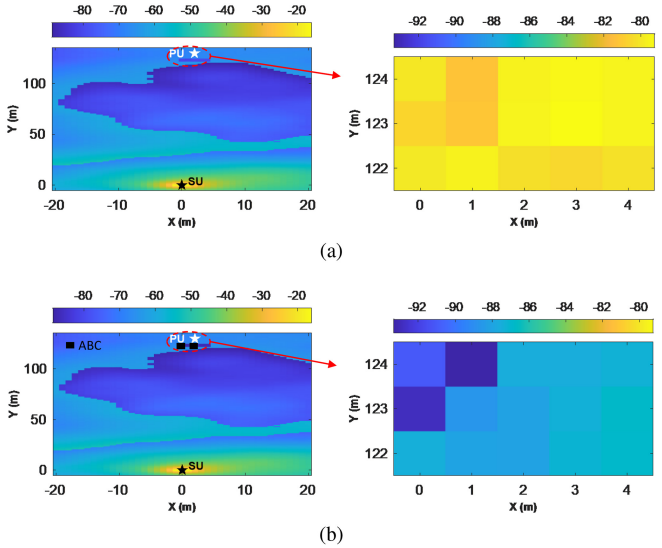

FIGURE 6. Demonstration of zone protection with proposed system architecture compared with conventional BS beamforming where the color map is scaled in dB. (a) Only BS beamforming antennas are optimized, (b) Proposed system architecture with multiple ABCs.

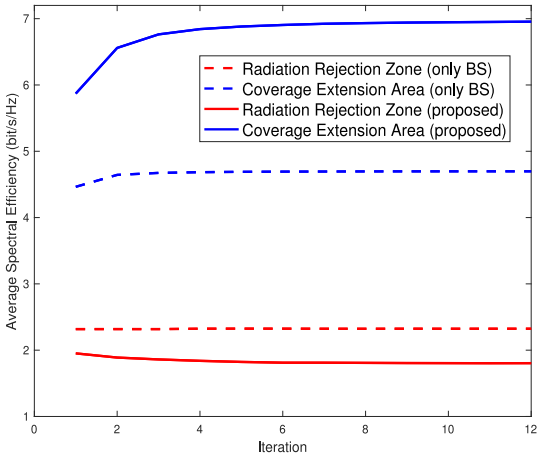

FIGURE 7. Convergence performance of the proposed method and its comparison with the case where RISs and ABCs are absent.

D. NUMERICAL RESULTS

The 2D topological color map in Fig. 6 shows the performance of multiple coordinated ABCs minimizing the signal power in encircled area in terms of dB. The SU is denoted as black star, where the PU is a white star. Multiple ABCs are denoted as black circles which are distributed around the protected zone. The detected radiation power in the encircled area by BS beamforming is shown in Fig. 6a, whereas the effect of multiple ABCs to suppress the interference is clearly observed (in colder color) in Fig. 6b. In the enlarged plots, initial usage of ABC achieves 12 dB reduction of the interference power in the rejection zone protecting primary system or its sensitive receiver. Although ambient backscatter nodes are just intuitively placed in the study, impressive degradation to form the radiation rejection zone is proven a disruptive but effective approach. Based on the rich literature about ABC, further explorations and exploitation can be conducted.

V. RADIATION CONTROL SYSTEM INCLUDING REPOSITIONABLE DYNAMIC RIS AND AMBIENT BACKSCATTER COMMUNICATION

In the existing literature, the RIS technology has been integrated into ambient backscatter communication system for performance improvement [40], [62]–[64]. In [62], the effect of the RIS on the source-to-reader and source-to-tag links of the ABC system is investigated with the bit-error rate (BER) performance indicator. Moreover, reference [63] studies advanced spatial multiplexing techniques of the RIS assisted ABC system by analytically showing that presence of the RIS can improve the spectral and energy efficiency. Experimental analysis of the RIS improved ABC system is performed in [64]. It is shown that pre-defined codebooks of the RIS can be selected according to the location of the ABC tag where its BER performance can be enhanced. The RIS-assisted MIMO symbiotic radio system is proposed in [40] where the RIS both enhance the primary transmission and embed the message acting like secondary transmission. In our work, the use multiple ABCs and the repositionable dynamic RIS in a coordinated manner is novelly proposed to control the electromagnetic radiation in 3D cognitive radio system.

In this section, the proposed ideas in Section III and Section IV are integrated into one system in order to control the whole electromagnetic radiation that is emitted from secondary BS. It is aimed that the radiation power in the vicinity of primary use is minimized which is called as radiation rejection zone, and at the same time, the whole radiation from secondary BS is steered to area where power of secondary use needs to be maximized.

Putting together both dynamic repositionable RISs and multiple ABCs into one systems to control the whole electromagnetic radiation in the environment, the problem formulation (P2) and (P3) can be revisited as follows:

$$
\begin{aligned}
\max_{\boldsymbol{\Theta}_{\mathrm{RIS}},\boldsymbol{\Theta}_{\mathrm{ABC}},\mathbf{W},\mathbf{Z}} \quad & \mathbb{E}\{\mathbf{R}'\} && (P4)\\
\text{s.t.} \quad & \left\|\mathbf{G}''\right\|^2 <= I \\
& \|\mathbf{W}\|^2 <= P \\
& \theta_{n_{\mathrm{BS}_k}} \in \mathcal{F}_{\mathrm{BS}}, 1 \le n_{\mathrm{BS}_k} \le N_{\mathrm{BS}_k} \\
& \theta_{n_{\mathrm{RIS}_k}} \in \mathcal{F}_{\mathrm{RIS}}, 1 \le n_{\mathrm{RIS}_k} \le N_{\mathrm{RIS}_k} \\
& (i,j)_k \in \mathsf{M} \\
& \left\|\boldsymbol{\Theta}_{\mathrm{ABC}_l}\right\|^2 <= P_l, \quad 1 \le l \le L \\
& \theta_{n_{\mathrm{ABC}_k}} \in \mathcal{F}_{\mathrm{A}}, 1 \le n_{\mathrm{ABC}_k} \le N_{\mathrm{ABC}_k} && (18)
\end{aligned}
$$

where I is the predefined interference power constraint in the vicinity of primary use. Problem (P4) has both non-convex objective function and constraints under the sets $\mathcal{F}_{\mathrm{BS}}, \mathcal{F}_{\mathrm{RIS}}, \mathcal{F}_{\mathrm{A}}$ similar to [65]. Monte Carlo method is used to eliminate the mathematical expectation in the objective

Algorithm 3 Alternating Optimization for (P3)

1: Initialize the all elements of $\mathbf{W}$ and $\boldsymbol{\Theta}_{\mathrm{ABC}_l}, \forall l = 1, \ldots, L$ with one.
2: **repeat**
3: **for** n $\leq N_{\mathrm{BS}} + \sum_l^L N_{\mathrm{ABC}}$ (total elements) **do**
4: Assign the corresponding phase shift value depending on the index j to the antenna i
5: Find the indices $\varsigma_{\mathrm{BS}} \in \boldsymbol{\varsigma}_{\mathrm{BS}}$ and $\varsigma_{\mathrm{ABC}_l} \in \boldsymbol{\varsigma}_{\mathrm{ABC}}$ that minimize the average channel gain of total M MPs, denoted as $\mathbf{G}''$
6: Assign the corresponding phase shift values depending on the index ς_{BS} or $\varsigma_{\mathrm{ABC}_l}$ to the corresponding antenna phase shifter n
7: **end for**
8: **until** Convergence is reached

function of (P4). Then alternating optimization method similar to Algorithm **2** and Algorithm **3** is employed to find sub-optimum solutions for $\boldsymbol{\Theta}_{\mathrm{RIS}}, \boldsymbol{\Theta}_{\mathrm{ABC}}, \mathbf{W}, \mathbf{Z}$.

It can be readily verified that the objective value of (P1) and (P2) monotonically increases with alternating optimization algorithm in each iteration where coverage has desired to be increased. In addition, due to the power constraints, the objective function has an upper bound. It is guaranteed to converge. Besides, the proposed algorithm can guarantee to yield a monotonically decreasing objective function value compared to the previous phase solution, i.e., $\boldsymbol{G}''(\boldsymbol{\Theta}_{\mathrm{ABC}})^{t+1} < \boldsymbol{G}''(\boldsymbol{\Theta}_{\mathrm{ABC}})^{t}$ for interference minimization in (P3) where t denotes the iteration number. The convergence performance of the proposed alternating optimization algorithm is presented in Fig. 7. Here, vertical axis demonstrates the average spectral efficiency overall MPs in the coverage extension area and radiation rejection zone due to secondary BS emission. It can be seen from Fig. 7 that the proposed algorithm converges for about 6 iterations. It can also be implied that the proposed structure enhances the spectral efficiency of coverage extension area of secondary use. At the same time, it can be implied that the proposed structure decreases the electromagnetic radiation of secondary use on the vicinity of primary use.

The coexistence of the repositionable dynamic RISs and multiple ABCs are studied in Fig. 8. The simulation parameters for BS, RIS and ABC are given in Table 1, as well. The dB scale color map shown in Fig. 8a is obtained by optimizing the antennas of secondary BS. On the other hand, the position repositionable dynamic RIS and phase shifts of ABCs and RISs antennas are optimized in the Fig. 8b. It can be seen that the signal power of secondary BS is enhanced around 10 dB in the coverage extension area. At the same time, the interference power in the vicinity of primary use can be rejected around 3 dB. The computational complexity of the proposed algorithms includes the multiplication of all possible selections for $\boldsymbol{\Theta}_{\mathrm{RIS}}, \boldsymbol{\Theta}_{\mathrm{ABC}}, \mathbf{W}, \mathbf{Z}$ depending on b_{RIS}, b_{ABC}, b_{BS} and the coordinates of grid points in the map M, which is relatively high and needs to be decreased to make proposed structure suitable for real test-bed.

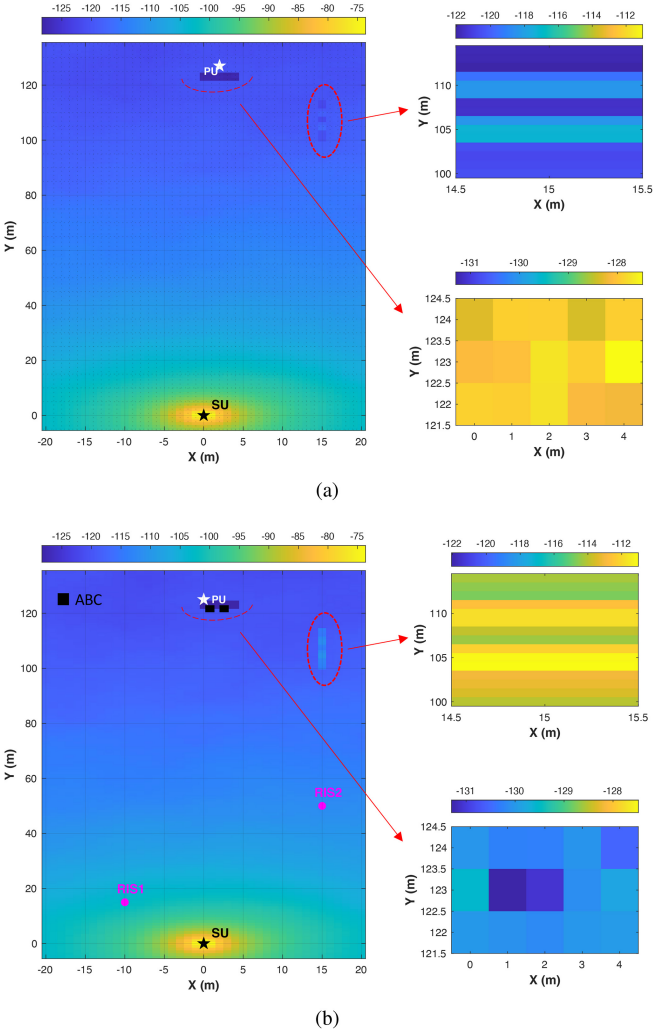

FIGURE 8. Demonstration of radiation control with repositionable dynamic RISs and multiple ABCs compared with only BS beamforming where the color map is scaled in dB. (a) Only BS beamforming applied, (b) proposed system architecture.

VI. MACHINE LEARNING TO FORM SPECTRUM MAP

One critical criterion to form a smart radio environment is to classify the permissible area(s) allowing co-existing radio communication. In this section, we propose to elaborate machine learning technique to better accomplish the goal.

A. STATE OF ART

One of the fundamental challenge of next wireless communications systems lies in the spectrum utilization with the increase in massive connectivity and various quality of service (QoS) requirements [66]. The spectrum availability (or utilization *vice versa*) indicated on the geographical map is known as *spectrum map*, which was initially realized by synthetic aperture radar [67] or compressive sensing [68]. Its application to cellular systems starts from cognitive radio resource allocation based on distributed sensing [11] in

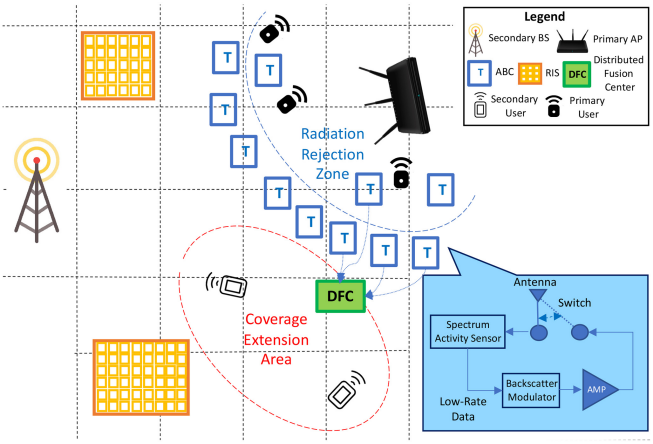

FIGURE 9. Spectrum activity sensor generates low-rate data that is transmitted via backscatter communication to distributed fusion center (DFC) so that edge AI can forecasts spectrum activities to dynamically adjust RISs.

3GPP R10. Cognitive radio network tomography further utilizes statistical inference to enable holistic understanding of spectrum activities [11]. Integrating both cognitive radio network tomography and spectrum map [70], the spectrum map can empower resource management for QoS guarantees [71] and opportunistic routing [72]. The amazing aspect of spectrum map is explained by Figure 1 to allow secondary systems geographically separated from primary systems, and thus achieve near ideal co-existing communication toward more efficient utilization of spectrum. maximum likelihood (ML) has been introduced to cooperative [73], non-cooperative [74], mobile [75], and spatio-temporal [76] spectrum sensing mechanisms. With the enhanced ML techniques, the intelligent spectrum sensing will play an essential role in co-existing radio networks [77]. A recent effort applies SVM to classify historical spectrum decision data to create the two-dimensional transmission opportunity map for a transmitter [78]. Both [79] and [80] take advantage of a number of distributed devices to facilitate intelligent wireless communication, which inspires ML to construct spectrum map.

B. SPECTRUM SENSORS APPLYING BACKSCATTER COMMUNICATIONS

Cooperative spectrum sensing has been proposed for a long time, which suffers the extra communication from sensors to the transmitter. The intuitive construction of spectrum map inevitably requires cooperative spectrum activity sensors but keeps the spatial spectrum efficiency as same. Synthetic aperture radar leveraging antenna array to construct spectrum map [67] can see through its coverage but not enough to establish the spectrum map for the entire region. Recalling the fact that each spectrum sensor only needs to transmit 1-bit information to construct the entire spectrum map [68], we again take advantage of ABC to form a smart spectrum sensor network toward the entire spectrum map as shown in Figure 9. As the blue box, a spectrum sensor senses the radio strength at certain frequency band(s) and translates into a short data packet, which the spectrum information is decoded into 1 (or just few) bit to well serve the purpose of spectrum map construction for any frequency band. Such small data packet can leverage ABC (with optional amplification depending on the operating needs) to be transmitted to a DFC when the RF switch turns to the transmission mode. By this way, the spectrum sensors can operate in a maintenance-free manner since such ABCs may utilize energy harvesting, which resolves the *device management* dilemma of sensor networks.

We may view the transmitter in Figure 9 as the BS or AP in the radio-access network (RAN) of the secondary system, which has an edge server to analyze the sensor data to (i) construct the spectrum map (ii) control the RISs accordingly and possibly move RIS dynamically. There are likely several DFCs in the intended radio coverage region and DFC has battery-operating communication and computational capability. These DFCs can (i) send data to BS to learn in a centralized manner, or (ii) exchange in an distributed ad hoc manner among them and BS, with privacy-preserving functionality.

C. SUPPORT VECTOR MACHINE TO CLASSIFY SPECTRUM MAP

Fundamentally, the construction of spectrum map based on the spectrum activity sensor data may proceed: hypothesis testing or statistical classification, and two-dimensional estimation or regression. Due to potential complex geometric property, statistical classification is considered. Different ML techniques toward cooperative spectrum sensing are investigated in wireless IoT, HetNets, MIMO, D2D and NOMA networks [81], [82]. Generally, cooperative spectrum sensing is to determine the transmission opportunity at a single geographical location for point-to-point cognitive radio communication. On the contrary, spectrum map to realize proposed multiple RISs technology provides the information to transmit the radio signals through a wide geographical area to serve multiple secondary co-existing users, much beyond a single point. After examining ML techniques [83], [84] and considering the fact that there lacks of stationary data to construct spectrum map that is designed for the need of dynamic radio channels including interference, SVM derived from statistical learning appears to meet our initial purpose with partially known models of communication systems. Also, SVM can even handle 1-bit sensor information to get satisfactory results, which is cumborsome for other ML techniques. Applying SVM to construct 2D or even 3D spectrum map has a fundamental difference from spectrum sensing for point-to-point communication, while adopting linearly separable SVM [85]. Even though spectrum sharing concept is studied for ABC networks in [86], how to obtain spectrum map and how to perform spectrum sensing via ABCs are not clear. Inspired by [87] where linear and nonlinear kernel SVM analysis for coverage boundary

detection are performed, this study explores ML aided spectrum map construction based on limited sensor information obtained via backscatter communication which is shown as efficient and thus helps to establish smart radio environment.

Mathematically, the spectrum activity data from nth sensor forms the sensor data vector $\mathbf{x}_n$. Based on the sensing spectrum value (e.g., radio signal strength, etc. at the target frequency band), the nth sensor can be classified as label y_n indicating suitability for secondary communication ($y_n = +1$) or unsuitability ($y_n = -1$) at its location. For each geographical location of interest, the BS of the secondary system must *predict* its label (i.e., $+1$ or -1). In a geographical area of the secondary co-existing system, a hyperplane $\mathbf{a}^T\mathbf{x} + b = 0$ to separate into a region ($+1$) and another region (-1). The goal of learning is to find $\mathbf{a}, b$. For a 2-D area, this hyperplane is actually a line in a *linearly separable* SVM classification problem. Unfortunately, such a solution is obviously useless for spectrum map. To resolve this dilemma, the SVM classification of spectrum map can be modified into the Lagrange multiplier version as

$$\mathcal{L} = \sum_{n=1}^{N} \lambda_n - \frac{1}{2} \sum_{i=1}^{N} \sum_{j=1}^{N} \lambda_i \lambda_j y_i y_j \mathbf{x}_i^T \mathbf{x}_j. \tag{19}$$

The equivalent problem is to maximize $\mathcal{L}$ over $\lambda_n \geq 0$, subject to $\sum_{n=1}^{N} \lambda_n y_n = 0$, which is known as the *dual problem*. Once we found the $\lambda_n, n = 1, \ldots, N$, the dual version of this classifier for a new data point $\mathbf{x}_{new}$ can be expressed as follows to classify H_1 and H_0 (i.e., permissible for co-existing secondary system to operate or not):

$$\sum_{n=1}^{N} \lambda_n y_n \mathbf{x}_n^T \mathbf{x}_{new} + b \underset{<}{>} 0. \tag{20}$$

The maximization of $\mathcal{L}$ will return almost all λ_n as zero. Those who are not zero correspond to the *support vectors* that define the margins. Furthermore, the problem can be extended into the soft-margin problem as follows:

$$\mathcal{J} = \frac{1}{N} \sum_{n=1}^{N} \max\Big[1 - y_n\Big(\mathbf{a}^T\mathbf{x}_n + b\Big), 0\Big] + \lambda \|\mathbf{a}\|^2, \tag{21}$$

where $\mathcal{J}$ consists of two terms which are loss function and regularization. λ plays the role of weighting between margin size and whether it lies on the correct side of the margin or not. Since $\mathcal{J}$ is convex in a, the (stochastic) gradient decent method is suitable for finding the solution. As shown in Figure 1, simple curve is still not enough for the desired co-existing utilization of spatial spectrum under complex propagation environments. Consequently, the radial basis function kernel, $K(\mathbf{x}, \mathbf{x}') = \exp(-\frac{\|\mathbf{x}-\mathbf{x}'\|^2}{2\sigma^2})$, also known as Gaussian kernel, is introduced. Furthermore, transmission from all sensors all the time consumes a lot of bandwidth. Therefore, each spectrum sensor shall decode the spectrum information into 1 bit (suitable for co-existing communication or not) according to compressed sensing [68].

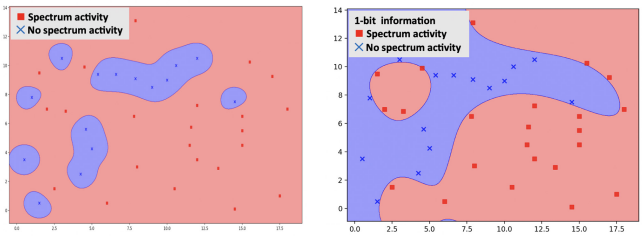

FIGURE 10. (Left) Reconstruction of spectrum based on 1-bit information of spectrum activity and conventional SVM using radical basis kernel, while red region indicates active operation of primary system. (Right) Successful construction of spectrum map to identify permission region (in blue) and active zone of primary system and the area requiring high radio rejection based on the refinement of SVM.

D. NUMERICAL RESULTS

There exists an advantage by 1-bit spectrum information: the spectrum sensors around the area requiring high radiation rejection, such as that for radio astronomy, measure low spectrum activity and the raw data can mislead the construction of spectrum availability map. A straightforward solution is to preset their values indicating unsuitable for co-existing communication, then using Gaussian kernel in (19).

As Figure 10(Left) showing the consequent construction of spectrum map, it successfully forms the spectrum map indicating permissible region (suitable for secondary co-existing communication, in blue); but is not possible for effective utilization while the original spatial spectrum allows a large connected region for RIS technology. It is not because the Gaussian kernel only considers squared Enclidean distance. Actually, Gaussian kernel equivalently considers higher order terms in inner product space to accommodate complex propagation channel dynamics. To resolve this challenge, further techniques are required. As SVM performance is sensitive to parameters, slack variables ζ_n are introduced for $\mathbf{x}_n, y_n$, the soft penalization $c_0 \sum_{n=1}^{N} \zeta_n + \frac{1}{2}\lambda\|\mathbf{a}\|^2$. Appropriate adjustment of parameters demonstrates accurate construction of spectrum map as shown in Figure 10 (Right).

VII. FUTURE RESEARCH DIRECTION AND CHALLANGES

Despite the many researches since the beginning of RIS and ABC studies, there are still promising open research problems, which need to be considered thoroughly. In the following part, some research directions and challenges related to our study are presented.

A. APPLICATION CENTRIC COEXISTING SMART RADIO

It is foreseen that 6G wireless systems will host much more diverse applications compared to 5G networks including holography, AR/VR assisted meta-verse, joint radar-sensing and communication, non-terrestrial networks, ultra-high speed railway networks. These networks will be in the same environment which are constantly interfering with each other. Repositionable dynamic RIS and multiple coordinated ABC assisted smart radio environment will be the remedy for highly overloaded future network in order to operate them in the minimal interference conditions since

our scheme provides 3D electromagnetic radiation control over the environment. As future works, specific networks needs to be studied regarding their waveforms, scheduling and used frequency bands to make the proposed smart radio environment concept suitable for standalone structures.

B. REAL TIME TEST-BED

Real time test-bed with repositionable dynamic RIS and multiple ABCs in different propagating environments needs to be studied rigorously. The test-bed should be designed to answer following critical questions: How can RISs and ABCs get the real-time channel estimation information to adjust their reflective elements? How will commands for the control of RISs and ABCs be declared in the real time? The development of EM-based repositionable dynamic RIS and ABC models and exploration of hardware imperfections/effects should be studied to make the proposed system feasible for next generation wireless communication systems.

C. REALISTIC AND SOPHISTICATED RIS, ABC AND OPTIMIZATION FRAMEWORKS

Robust optimization of resource allocation schemes is required in spatial, temporal and spectral domains. It includes the optimal position of multiple repositionable dynamic RISs and cross-coordinated optimization of the overall network including ABCs. The phase and amplitude arrangement of ABCs regarding the channel conditions of protected area and secondary user needs computationally efficient optimization. RIS-empowered PHY slicing which can support different applications such as wireless charging, PHY security and data transfer having passive, active and transmissive subsurfaces are introduced in [88]. Such a concept can be generalized by levering our ML-based spectrum mapping and multiple coordinated ABCs frameworks to make coexisting smart radio environment more sophisticated and mission critical.

D. PERFORMANCE LIMITS OF RIS AND ABC ASSISTED NETWORKS

Placement of these ambient backscatter nodes to fade the radiation from secondary co-existing systems can be a critical extension in case knowing the location of BS and RISs. Further robust placement without precise knowledge of BS and RIS, simply based on the required radiation (spatial-spectrum) rejection from the secondary system, serves the ultimate goal. Calculation and proof of essential performance limits of RIS and ABC assisted networks are needed.

E. FEDERATED LEARNING TO MANAGE SPECTRUM MAP

Once DFC obtain data from spectrum sensors, the learning to classify can be facilitated in two possible architecture, (i) hierarchical architecture such that DFCs send the data to the BS for centralized learning then constructing spectrum map; (ii) ad hoc architecture such that DFCs and BS exchange data in an ad hoc manner for distributed learning and constructing spectrum map. One of the purposes for distributed architecture is to avoid longer distance transmission consuming a lot of spatial spectrum. For the purpose of spatial bandwidth efficiency and privacy-preserving for data, a disruptive application of federated learning (FL) [89] is proposed for spectrum map construction. Instead of transmitting the data, stochastic gradient descent (SGD) parameters of SVM can be relayed either hierarchically or in ad hoc manner. This falls into the vertical FL [89]. Only exchange learning parameters rather than data of spectrum sensing data further minimizes spectrum use for co-existing systems while achieving privacy-preserving and cybersecurity against data interception. Pros and cons by FL, compared with traditional sensor data transmission, needs to be exploited using single- or multi-channel parallel transmission for further studies.

F. TOTAL ENERGY CONSUMPTION AND COST OF RIS AND ABC

With the increasing number of ABC nodes, the collaborative mechanism among ABCs and repositionable dynamic RISs should be investigated to enhance collective performance, given the energy and implementation constraints of ABC nodes. The amount of additional energy consumption should be investigated due to the positioning of RISs to find the optimum location.

VIII. CONCLUSION

This study novelly introduces a smart radio environment that shapes the electromagnetic energy in the spatial domain using channel control mechanisms such as repositionable dynamic RISs and multiple coordinated ABCs which is analogous to pulse shaping in time and frequency domain. We've started by investigating the advantage of multiple static RIS to increase the coverage area of secondary users. Then, we've added a novel property to RIS concept, which called repositionable dynamic RIS, providing more robustness to shadowing and power fluctuations in short time frame. It is shown that the proposed concept introduces 15% more coverage to the secondary systems. Finally, multiple ABCs are utilized to create radiation rejection zone for the use of primary user. The performance of proposed structure is demonstrated with 2D intensity maps. Also, ML-assisted spatial spectrum activity on the geographical map is demonstrated utilizing ABC sensors to manage the use of repositionable dynamic RISs. Combining these phenomena, pulse shaping like spatial domain electromagnetic radiation control concept is created. Regarding further studies, efficient optimization schemes and real time test bed experiments are needed to improve the feasibility of the idea.

ACKNOWLEDGMENT

The authors would like thank the anonymous reviewers and the editor for their insightful comments and suggestions that improves the quality of paper, as well as Hazal Dogukan, for her valuable help on drawing the figure to make the scheme more comprehensible.

REFERENCES

[1] G. Liu *et al.*, "Coverage enhancement and fundamental performance of 5G: Analysis and field trial," *IEEE Commun. Mag.*, vol. 57, no. 6, pp. 126–131, Jun. 2019.

[2] M. Giordani, M. Polese, M. Mezzavilla, S. Rangan, and M. Zorzi, "Toward 6G networks: Use cases and technologies," *IEEE Commun. Mag.*, vol. 58, no. 3, pp. 55–61, Mar. 2020.

[3] Y. Chen, P. Zhu, G. He, X. Yan, H. Baligh, and J. Wu, "From connected people, connected things, to connected intelligence," in *Proc. 2nd 6G Wireless Summit (6G SUMMIT)*, 2020, pp. 1–7.

[4] I. F. Akyildiz, A. Kak, and S. Nie, "6G and beyond: The future of wireless communications systems," *IEEE Access*, vol. 8, pp. 133995–134030, 2020.

[5] K.-C. Chen, S.-C. Lin, J.-H. Hsiao, C.-H. Liu, A. F. Molisch, and G. P. Fettweis, "Wireless networked multirobot systems in smart factories," *Proc. IEEE*, vol. 109, no. 4, pp. 468–494, Apr. 2021.

[6] H. Arslan, S. D. Tusha, and A. Yazar, "6G vision: An ultra-flexible perspective," *ITU J. Future Evol. Technol.*, vol. 1, no. 1, pp. 121–140, 2020.

[7] S. J. Nawaz, S. K. Sharma, S. Wyne, M. N. Patwary, and M. Asaduzzaman, "Quantum machine learning for 6G communication networks: State-of-the-art and vision for the future," *IEEE Access*, vol. 7, pp. 46317–46350, 2019.

[8] Z. Zhang *et al.*, "6G wireless networks: Vision, requirements, architecture, and key technologies," *IEEE Veh. Technol. Mag.*, vol. 14, no. 3, pp. 28–41, Sep. 2019.

[9] N. Rajatheva *et al.*, *White Paper on Broadband Connectivity in 6G*, vol. 10, 6G Res. Vis., Oulu, Finland, Apr. 2020, p. 1.

[10] J. Mitola and G. Q. Maguire, "Cognitive radio: Making software radios more personal," *IEEE Pers. Commun.*, vol. 6, no. 4, pp. 13–18, Aug. 1999.

[11] S.-Y. Lien, K.-C. Chen, Y.-C. Liang, and Y. Lin, "Cognitive radio resource management for future cellular networks," *IEEE Wireless Commun.*, vol. 21, no. 1, pp. 70–79, Feb. 2014.

[12] Y.-C. Liang, K.-C. Chen, G. Y. Li, and P. Mahonen, "Cognitive radio networking and communications: An overview," *IEEE Trans. Veh. Technol.*, vol. 60, no. 7, pp. 3386–3407, Sep. 2011.

[13] T. Yucek and H. Arslan, "A survey of spectrum sensing algorithms for cognitive radio applications," *IEEE Commun. Surveys Tuts.*, vol. 11, no. 1, pp. 116–130, 1st Quart., 2009.

[14] A. Martin, S. Harbison, and K. Beach, *An Introduction to Radiation Protection*. Boca Raton, FL, USA: CRC Press, 2019.

[15] M. Di Renzo *et al.*, "Smart radio environments empowered by reconfigurable AI meta-surfaces: An idea whose time has come," *EURASIP J. Wireless Commun. Netw.*, vol. 2019, p. 129, May 2019.

[16] M. Di Renzo *et al.*, "Smart radio environments empowered by reconfigurable intelligent surfaces: How it works, state of research, and the road ahead," *IEEE J. Sel. Areas Commun.*, vol. 38, no. 11, pp. 2450–2525, Nov. 2020.

[17] A. Welkie, L. Shangguan, J. Gummeson, W. Hu, and K. Jamieson, "Programmable radio environments for smart spaces," in *Proc. 16th ACM Workshop Hot Topics Netw.*, 2017, pp. 36–42.

[18] K.-K. Wong, K.-F. Tong, Z. Chu, and Y. Zhang, "A vision to smart radio environment: Surface wave communication superhighways," *IEEE Wireless Commun.*, vol. 28, no. 1, pp. 112–119, Feb. 2021.

[19] E. Basar, M. Di Renzo, J. De Rosny, M. Debbah, M.-S. Alouini, and R. Zhang, "Wireless communications through reconfigurable intelligent surfaces," *IEEE Access*, vol. 7, pp. 116753–116773, 2019.

[20] Q. Wu and R. Zhang, "Towards smart and reconfigurable environment: Intelligent reflecting surface aided wireless network," *IEEE Commun. Mag.*, vol. 58, no. 1, pp. 106–112, Jan. 2020.

[21] N. Van Huynh, D. T. Hoang, X. Lu, D. Niyato, P. Wang, and D. I. Kim, "Ambient backscatter communications: A contemporary survey," *IEEE Commun. Surveys Tuts.*, vol. 20, no. 4, pp. 2889–2922, 4th Quart., 2018.

[22] Y. Niu, Y. Li, D. Jin, L. Su, and A. V. Vasilakos, "A survey of millimeter wave communications (mmWave) for 5G: Opportunities and challenges," *Wireless Netw.*, vol. 21, no. 8, pp. 2657–2676, 2015.

[23] D. Lockie and D. Peck, "High-data-rate millimeter-wave radios," *IEEE Microw. Mag.*, vol. 10, no. 5, pp. 75–83, Aug. 2009.

[24] B. Mondal *et al.*, "3D channel model in 3GPP," *IEEE Commun. Mag.*, vol. 53, no. 3, pp. 16–23, Mar. 2015.

[25] I. A. Hemadeh, K. Satyanarayana, M. El-Hajjar, and L. Hanzo, "Millimeter-wave communications: Physical channel models, design considerations, antenna constructions, and link-budget," *IEEE Commun. Surveys Tuts.*, vol. 20, no. 2, pp. 870–913, 2nd Quart., 2018.

[26] M. Alayasra and H. Arslan, "IRS-enabled beam-space channel," *IEEE Trans. Wireless Commun.*, early access, Nov. 15, 2021, doi: 10.1109/TWC.2021.3124288.

[27] Ö. Özdogan, E. Björnson, and E. G. Larsson, "Intelligent reflecting surfaces: Physics, propagation, and pathloss modeling," *IEEE Wireless Commun. Lett.*, vol. 9, no. 5, pp. 581–585, May 2020.

[28] E. Björnson, Ö. Özdogan, and E. G. Larsson, "Intelligent reflecting surface versus decode-and-forward: How large surfaces are needed to beat relaying?" *IEEE Wireless Commun. Lett.*, vol. 9, no. 2, pp. 244–248, Feb. 2020.

[29] A. Taha, M. Alrabeiah, and A. Alkhateeb, "Enabling large intelligent surfaces with compressive sensing and deep learning," *IEEE Access*, vol. 9, pp. 44304–44321, 2021.

[30] Q.-U.-A. Nadeem, H. Alwazani, A. Kammoun, A. Chaaban, M. Debbah, and M.-S. Alouini, "Intelligent reflecting surface-assisted multi-user MISO communication: Channel estimation and beamforming design," *IEEE Open J. Commun. Soc.*, vol. 1, pp. 661–680, 2020.

[31] B. Zheng and R. Zhang, "Intelligent reflecting surface-enhanced OFDM: Channel estimation and reflection optimization," *IEEE Wireless Commun. Lett.*, vol. 9, no. 4, pp. 518–522, Apr. 2020.

[32] A. Goldsmith, *Wireless Communications*. New York, NY, USA: Cambridge Univ. Press, 2005.

[33] E. Basar and I. Yildirim, "Reconfigurable intelligent surfaces for future wireless networks: A channel modeling perspective," *IEEE Wireless Commun.*, vol. 28, no. 3, pp. 108–114, Jun. 2021.

[34] K. Haneda, "5G 3GPP-like channel models for outdoor urban microcellular and macrocellular environments," in *Proc. IEEE 83rd Veh. Technol. Conf. (VTC Spring)*, 2016, pp. 1–7.

[35] H. Guo, Y.-C. Liang, J. Chen, and E. G. Larsson, "Weighted sum-rate maximization for reconfigurable intelligent surface aided wireless networks," *IEEE Trans. Wireless Commun.*, vol. 19, no. 5, pp. 3064–3076, May 2020.

[36] C. Pan *et al.*, "Multicell MIMO communications relying on intelligent reflecting surfaces," *IEEE Trans. Wireless Commun.*, vol. 19, no. 8, pp. 5218–5233, Aug. 2020.

[37] C. A. Balanis, *Antenna Theory: Analysis and Design*. Hoboken, NJ, USA: Wiley, 2016.

[38] S. Ju, O. Kanhere, Y. Xing, and T. S. Rappaport, "A millimeter-wave channel simulator NYUSIM with spatial consistency and human blockage," in *Proc. IEEE Global Commun. Conf. (GLOBECOM)*, 2019, pp. 1–6.

[39] S. Li, B. Duo, X. Yuan, Y.-C. Liang, and M. Di Renzo, "Reconfigurable intelligent surface assisted UAV communication: Joint trajectory design and passive beamforming," *IEEE Wireless Commun. Lett.*, vol. 9, no. 5, pp. 716–720, May 2020.

[40] Q. Zhang, Y.-C. Liang, and H. V. Poor, "Reconfigurable intelligent surface assisted MIMO symbiotic radio networks," *IEEE Trans. Commun.*, vol. 69, no. 7, pp. 4832–4846, Jul. 2021.

[41] Y. Cao, T. Lv, and W. Ni, "Intelligent reflecting surface aided multi-user mmWave communications for coverage enhancement," in *Proc. IEEE 31st Annu. Int. Symp. Personal Indoor Mobile Radio Commun.*, 2020, pp. 1–6.

[42] R. Alghamdi *et al.*, "Intelligent surfaces for 6G wireless networks: A survey of optimization and performance analysis techniques," *IEEE Access*, vol. 8, pp. 202795–202818, 2020.

[43] C. Huang, A. Zappone, G. C. Alexandropoulos, M. Debbah, and C. Yuen, "Reconfigurable intelligent surfaces for energy efficiency in wireless communication," *IEEE Trans. Wireless Commun.*, vol. 18, no. 8, pp. 4157–4170, Aug. 2019.

[44] Q. Zhang, W. Saad, and M. Bennis, "Reflections in the sky: Millimeter wave communication with UAV-carried intelligent reflectors," in *Proc. IEEE Global Commun. Conf. (GLOBECOM)*, 2019, pp. 1–6.

[45] H.-L. Chiang, K.-C. Chen, W. Rave, M. K. Marandi, and G. Fettweis, "Multi-UAV mmWave beam tracking using Q-learning and interference mitigation," in *Proc. IEEE Int. Conf. Commun. Workshops (ICC Workshops)*, 2020, pp. 1–7.

[46] S. Alfattani *et al.*, "Aerial platforms with reconfigurable smart surfaces for 5G and beyond," *IEEE Commun. Mag.*, vol. 59, no. 1, pp. 96–102, Jan. 2021.

[47] L. Ge, P. Dong, H. Zhang, J.-B. Wang, and X. You, "Joint beamforming and trajectory optimization for intelligent reflecting surfaces-assisted UAV communications," *IEEE Access*, vol. 8, pp. 78702–78712, 2020.

[48] K. W. Cho, M. H. Mazaheri, J. Gummeson, O. Abari, and K. Jamieson, "mmWall: A reconfigurable metamaterial surface for mmWave networks," in *Proc. 22nd Int. Workshop Mobile Comput. Syst. Appl.*, 2021, pp. 119–125.

[49] M. H. Yılmaz, E. Güvenkaya, G. Mumcu, and H. Arslan, "Millimeter-wave wireless channel control using spatially adaptive antenna arrays," *IEEE Commun. Lett.*, vol. 21, no. 3, pp. 680–683, Mar. 2017.

[50] J. Mendoza, M. Karabacak, H. Arslan, and G. Mumcu, "A spatially adaptive antenna array for mm-wave wireless channel control with microfluidics based reconfiguration," *IEEE Access*, vol. 8, pp. 182898–182907, 2020.

[51] E. Basar, I. Yildirim, and F. Kilinc, "Indoor and outdoor physical channel modeling and efficient positioning for reconfigurable intelligent surfaces in mmWave bands," *IEEE Trans. Commun.*, vol. 69, no. 12, pp. 8600–8611, Dec. 2021.

[52] J. Li, "LOS probability modeling for 5G indoor scenario," in *Proc. Int. Symp. Antennas Propag. (ISAP)*, 2016, pp. 204–205.

[53] A. Bereketli and O. B. Akan, "Communication coverage in wireless passive sensor networks," *IEEE Commun. Lett.*, vol. 13, no. 2, pp. 133–135, Feb. 2009.

[54] V. Liu, A. Parks, V. Talla, S. Gollakota, D. Wetherall, and J. R. Smith, "Ambient backscatter: Wireless communication out of thin air," *SIGCOMM Comput. Commun. Rev.*, vol. 43, no. 4, pp. 39–50, Aug. 2013.

[55] W. Liu, Y.-C. Liang, Y. Li, and B. Vucetic, "Backscatter multiplicative multiple-access systems: Fundamental limits and practical design," *IEEE Trans. Wireless Commun.*, vol. 17, no. 9, pp. 5713–5728, Sep. 2018.

[56] H. Guo, Y.-C. Liang, R. Long, and Q. Zhang, "Cooperative ambient backscatter system: A symbiotic radio paradigm for passive IoT," *IEEE Wireless Commun. Lett.*, vol. 8, no. 4, pp. 1191–1194, Aug. 2019.

[57] H. Guo, R. Long, and Y.-C. Liang, "Cognitive backscatter network: A spectrum sharing paradigm for passive IoT," *IEEE Wireless Commun. Lett.*, vol. 8, no. 5, pp. 1423–1426, Oct. 2019.

[58] M. A. ElMossallamy, M. Pan, R. Jäntti, K. G. Seddik, G. Y. Li, and Z. Han, "Noncoherent backscatter communications over ambient OFDM signals," *IEEE Trans. Commun.*, vol. 67, no. 5, pp. 3597–3611, May 2019.

[59] Y.-C. Liang, Q. Zhang, E. G. Larsson, and G. Y. Li, "Symbiotic radio: Cognitive backscattering communications for future wireless networks," *IEEE Trans. Cogn. Commun. Netw.*, vol. 6, no. 4, pp. 1242–1255, Dec. 2020.

[60] "AWMF-0108—n257/n261 Band Quad Core IC." [Online]. Available: https://www.anokiwave.com/products/awmf-0108/index.html (Accessed: Nov. 15, 2021).

[61] S. S. Rao, *Introduction to Optimization*. Hoboken, NJ, USA: Wiley, 2019. [Online]. Available: https://onlinelibrary.wiley.com/doi/abs/10.1002/9781119454816.ch1

[62] Y. Chen, "Performance of ambient backscatter systems using reconfigurable intelligent surface," *IEEE Commun. Lett.*, vol. 25, no. 8, pp. 2536–2539, Aug. 2021.

[63] A. Bhowal, S. Aïssa, and R. S. Kshetrimayum, "RIS-assisted advanced spatial modulation techniques for ambient backscattering communications," *IEEE Trans. Green Commun. Netw.*, vol. 5, no. 4, pp. 1684–1696, Dec. 2021.

[64] R. Fara, D.-T. Phan-Huy, P. Ratajczak, A. Ourir, M. Di Renzo, and J. De Rosny, "Reconfigurable intelligent surface-assisted ambient backscatter communications—Experimental assessment," in *Proc. IEEE Int. Conf. Commun. Workshops (ICC Workshops)*, 2021, pp. 1–7.

[65] J. Hu, Y.-C. Liang, and Y. Pei, "Reconfigurable intelligent surface enhanced multi-user MISO symbiotic radio system," *IEEE Trans. Commun.*, vol. 69, no. 4, pp. 2359–2371, Apr. 2021.

[66] P. Cheng, Z. Chen, M. Ding, Y. Li, B. Vucetic, and D. Niyato, "Spectrum intelligent radio: Technology, development, and future trends," *IEEE Commun. Mag.*, vol. 58, no. 1, pp. 12–18, Jan. 2020.

[67] T.-W. Chiang and K.-C. Chen, "Synthetic aperture radar construction of spectrum map for cognitive radio networking," in *Proc. 6th Int. Wireless Commun. Mobile Comput. Conf.*, New York, NY, USA, 2010, pp. 631–635.

[68] S.-Y. Shih and K.-C. Chen, "Compressed sensing construction of spectrum map for routing in cognitive radio networks," in *Proc. IEEE 73rd Veh. Technol. Conf. (VTC Spring)*, 2011, pp. 1–5.

[69] C.-K. Yu, K.-C. Chen, and S.-M. Cheng, "Cognitive radio network tomography," *IEEE Trans. Veh. Technol.*, vol. 59, no. 4, pp. 1980–1997, May 2010.

[70] C.-K. Yu and K.-C. Chen, "Spectrum map retrieval using cognitive radio network tomography," in *Proc. IEEE GLOBECOM Workshops (GC Wkshps)*, 2011, pp. 986–991.

[71] S.-Y. Lien, S.-Y. Shih, and K.-C. Chen, "Spectrum map empowered resource management for QoS guarantees in multi-tier cellular networks," in *Proc. IEEE Global Telecommun. Conf. (GLOBECOM)*, 2011, pp. 1–6.

[72] S.-C. Lin and K.-C. Chen, "Spectrum-map-empowered opportunistic routing for cognitive radio ad hoc networks," *IEEE Trans. Veh. Technol.*, vol. 63, no. 6, pp. 2848–2861, Jul. 2014.

[73] W. Lee, M. Kim, and D.-H. Cho, "Deep cooperative sensing: Cooperative spectrum sensing based on convolutional neural networks," *IEEE Trans. Veh. Technol.*, vol. 68, no. 3, pp. 3005–3009, Mar. 2019.

[74] B. M. Pati, M. Kaneko, and A. Taparugssanagorn, "A deep convolutional neural network based transfer learning method for non-cooperative spectrum sensing," *IEEE Access*, vol. 8, pp. 164529–164545, 2020.

[75] Y. Xu, P. Cheng, Z. Chen, Y. Li, and B. Vucetic, "Mobile collaborative spectrum sensing for heterogeneous networks: A Bayesian machine learning approach," *IEEE Trans. Signal Process.*, vol. 66, no. 21, pp. 5634–5647, Nov. 2018.

[76] O. P. Awe, A. Deligiannis, and S. Lambotharan, "Spatio-temporal spectrum sensing in cognitive radio networks using beamformer-aided SVM algorithms," *IEEE Access*, vol. 6, pp. 25377–25388, 2018.

[77] Z. Qin and G. Y. Li, "Pathway to intelligent radio," *IEEE Wireless Commun.*, vol. 27, no. 1, pp. 9–15, Feb. 2020.

[78] X.-L. Huang, Y. Gao, X.-W. Tang, and S.-B. Wang, "Spectrum mapping in large-scale cognitive radio networks with historical spectrum decision results learning," *IEEE Access*, vol. 6, pp. 21350–21358, 2018.

[79] H. Joshi, S. Santra, S. J. Darak, M. K. Hanawal, and S. V. S. Santosh, "Multiplay multiarmed bandit algorithm based sensing of noncontiguous wideband spectrum for AIoT networks," *IEEE Trans. Ind. Informat.*, vol. 18, no. 5, pp. 3337–3348, May 2022.

[80] L. Li and A. Ghasemi, "IoT-enabled machine learning for an algorithmic spectrum decision process," *IEEE Internet Things J.*, vol. 6, no. 2, pp. 1911–1919, Apr. 2019.

[81] F. Hussain, S. A. Hassan, R. Hussain, and E. Hossain, "Machine learning for resource management in cellular and IoT networks: Potentials, current solutions, and open challenges," *IEEE Commun. Surveys Tuts.*, vol. 22, no. 2, pp. 1251–1275, 2nd Quart., 2020.

[82] K. M. Thilina, K. W. Choi, N. Saquib, and E. Hossain, "Machine learning techniques for cooperative spectrum sensing in cognitive radio networks," *IEEE J. Sel. Areas Commun.*, vol. 31, no. 11, pp. 2209–2221, Nov. 2013.

[83] C. Jiang, H. Zhang, Y. Ren, Z. Han, K.-C. Chen, and L. Hanzo, "Machine learning paradigms for next-generation wireless networks," *IEEE Wireless Commun.*, vol. 24, no. 2, pp. 98–105, Apr. 2017.

[84] J. Wang, C. Jiang, H. Zhang, Y. Ren, K.-C. Chen, and L. Hanzo, "Thirty years of machine learning: The road to Pareto-optimal wireless networks," *IEEE Commun. Surveys Tuts.*, vol. 22, pp. 1472–1514, 3rd Quart., 2020.

[85] Y. Qi, Y. Wang, and C. Lai, "An improved SVM-based spatial spectrum sensing scheme via beamspace at low SNRs," *IEEE Access*, vol. 7, pp. 184759–184768, 2019.

[86] Q. Wang, H. Sun, R. Q. Hu, and A. Bhuyan, "When machine learning meets spectrum sharing security: Methodologies and challenges," *IEEE Open J. Commun. Soc.*, vol. 3, pp. 176–208, 2022.

[87] G. Ding, Q. Wu, Y.-D. Yao, J. Wang, and Y. Chen, "Kernel-based learning for statistical signal processing in cognitive radio networks: Theoretical foundations, example applications, and future directions," *IEEE Signal Process. Mag.*, vol. 30, no. 4, pp. 126–136, Jul. 2013.

[88] E. Basar and H. V. Poor, "Present and future of reconfigurable intelligent surface-empowered communications [perspectives]," *IEEE Signal Process. Mag.*, vol. 38, no. 6, pp. 146–152, Nov. 2021.
[89] Q. Yang, Y. Liu, T. Chen, and Y. Tong, "Federated machine learning: Concept and applications," *ACM Trans. Intell. Syst. Technol.*, vol. 10, no. 2, pp. 1–19, 2019.

MEHMET MERT ŞAHIN (Graduate Student Member, IEEE) received the B.S. degree from Bilkent University, Ankara, Turkey, in 2019. He is currently pursuing the Ph.D. degree with the University of South Florida, Tampa, FL, USA. He worked with Aselsan Inc. as a Wireless Communication Design Engineer in 2019. His research interest include waveform design for future wireless networks, multiple accessing, interference management, joint radar-sensing, and communication.

HÜSEYIN ARSLAN (Fellow, IEEE) received the B.S. degree from Middle East Technical University, Ankara, Turkey, in 1992, and the M.S. and Ph.D. degrees from Southern Methodist University, Dallas, TX, USA, in 1994 and 1998, respectively. From 1998 to 2002, he was with the Research Group, Ericsson Inc., Morrisville, NC, USA, where he was involved with several projects related to 2G and 3G wireless communication systems. Since 2002, he has been with the Electrical Engineering Department, University of South Florida, Tampa, FL, USA. In December 2013, he joined Istanbul Medipol University to found the Engineering College, where he has worked as the Dean of the School of Engineering and Natural Sciences. In addition, he has worked as a part-time Consultant for various companies and institutions, including Anritsu Company and the Scientific and Technological Research Council of Turkey. He has been collaborating extensively with key national and international industrial partners and his research has generated significant interest in companies, such as InterDigital, Anritsu, NTT DoCoMo, Raytheon, Honeywell, and Keysight Technologies. Collaborations. He conducts research in wireless systems, with emphasis on the physical and medium access layers of communications. His current research interests include 5G and beyond radio access technologies, physical layer security, interference management (avoidance, awareness, and cancellation), cognitive radio, multi-carrier wireless technologies (beyond OFDM), dynamic spectrum access, co-existence issues, non-terrestrial communications (high altitude platforms), joint radar (sensing), and communication designs. He has served as a technical program committee member, the general chair, the technical program committee chair, a session and symposium organizer, and the workshop chair for several IEEE conferences. He has also served as a member of the Editorial Board for the IEEE TRANSACTIONS ON COMMUNICATIONS, the IEEE TRANSACTIONS ON COGNITIVE COMMUNICATIONS AND NETWORKING, and several other scholarly journals by Elsevier, Hindawi, and Wiley Publishing. He is a member of the Editorial Board for the IEEE COMMUNICATIONS SURVEYS AND TUTORIALS and the *Sensors*.

KWANG-CHENG CHEN (Fellow, IEEE) received the B.S. degree in electrical engineering from National Taiwan University, Taipei, Taiwan, in 1983, and the M.S. and Ph.D. degrees in electrical engineering from the University of Maryland, College Park, USA, in 1987 and 1989, respectively. From 1987 to 1998, he worked with SSE, COMSAT, IBM Thomas J. Watson Research Center, and National Tsing Hua University. From 1998 to 2016, he was a Distinguished Professor with National Taiwan University also served as the Director of Graduate Institute of Communication Engineering, the Director of Communication Research Center, and the Associate Dean for Academic Affairs with the College of Electrical Engineering and Computer Science from 2009 to 2015. Since 2016, he has been a Professor of Electrical Engineering with the University of South Florida, Tampa, FL, USA. His recent research interests include wireless networks, multi-robot systems and machine learning, quantum information systems and cybersecurity, and social networks. He has received the number of awards, including the 2011 IEEE COMSOC WTC Recognition Award, the 2014 IEEE Jack Neubauer Memorial Award, and the 2014 IEEE COMSOC AP Outstanding Paper Award. He has been actively involving in the organization of various IEEE conferences as General/TPC chair/co-chair and has served in editorships with a few IEEE journals. He also actively participates in and has contributed essential technology to various IEEE 802, Bluetooth, LTE and LTE-A, 5G-NR, and ITU-T FG ML5G wireless standards.